From DEPARTMENT OF CLINICAL NEUROSCIENCE
Karolinska Institutet, Stockholm, Sweden

RETINAL THICKNESS MEASURED WITH OPTICAL COHERENCE TOMOGRAPHY IN PATIENTS WITH MULTIPLE SCLEROSIS

Ulrika Birkeldh

Karolinska Institutet

Stockholm 2018

Published by Karolinska Institutet.
Printed by Eprint AB 2018

ISBN 978-91-7831-052-4

RETINAL THICKNESS MEASURED WITH OPTICAL COHERENCE TOMOGRAPHY IN PATIENTS WITH MULTIPLE SCLEROSIS
THESIS FOR DOCTORAL DEGREE (Ph.D.)

By

Ulrika Birkeldh

Principal Supervisor:
Associate Professor Rune Brautaset
Karolinska Institutet
Department of Clinical Neuroscience
Division of Eye and Vision

Co-supervisor(s):
PhD Maria Nilsson
Karolinska Institutet
Department of Clinical Neuroscience
Division of Eye and Vision

PhD Marika Wahlberg Ramsay
Karolinska Institutet
Department of Clinical Neuroscience
Division of Eye and Vision

MD/PhD Max Albert Hietala
Karolinska Institutet
Department of Clinical Neuroscience
Division of Neuro

PhD Ali Manouchehrinia
Karolinska Institutet
Department of Clinical Neuroscience
Division of Neuro

Opponent:
Professor Jan Richard Bruenech
University College of South-Eastern Norway
Department of Optometry, Radiography and Lighting Design

Examination Board:
Associate Professor Marcelo Ayala
University of Gothenburg
Institute of Neuroscience and Physiology
Department of Clinical Neuroscience

Professor Michael Larsen
University of Copenhagen
Glostrup Hospital
Department of Ophthalmology

Professor Anne-Marie Landtblom
Uppsala University
Department of Neuroscience
Division of Neurology

To my family

ABSTRACT

The retina offers a unique window to the brain with its unmyelinated axons that converge to the optic nerve. Optical coherence tomography (OCT) is a well-established and non-invasive imaging technique in the ophthalmology field. The retinal layers can be imaged directly, and OCT is often described as an optical biopsy of retinal tissue. OCT has many practical advantages, as ease of use, short acquisition time and being relatively inexpensive. During the past decade the interest in OCT has grown in the neurology field and its potentials as an imaging modality that might complement magnetic resonance imaging (MRI). Multiple sclerosis is a complex chronic neurological disease that leads to both gray and white matter damage. OCT has shown promising results in several studies focusing on MS and neurodegeneration in the brain.

Paper 1 evaluated the repeatability of images taken by Canon OCT-HS100 with the new automatic eye track function. The results showed good correlation with the well-established Zeiss Cirrus HD-OCT 5000, however it was clear that OCTs are not interchangeable due to differences in thickness estimations. Paper 2 confirmed in a large MS cohort, findings from previous studies that the peripapillary retinal nerve fiber layer (pRNFL) is reduced in eyes of MS patients compared with healthy controls (HCs), regardless of optic neuritis (ON) history. The temporal quadrant of pRNFL (T-pRNFL) demonstrated the strongest correlation to both physical disability, assessed with the Expanded Disability Status Scale (EDSS) and cognitive impairment, measured with Symbol Digit Modalities Test (SDMT). Paper 3 aimed to evaluate different OCT parameters in MS patients and investigate which might best describe physical disability and cognitive impairment. All of four included OCT measures showed a statistically significant thickness reduction in MS eyes compared with HCs. The T-pRNFL of primary progressive MS patients had the largest atrophy of the inner retinal layers compared with HCs. The EDSS showed a strong and significant inverse correlation with all four OCT measures. SDMT had the strongest correlation with average pRNFL and T-pRNFL thicknesses.

In conclusion, OCT is a sensitive method to assess structural damage of neurons and their axons in the visual pathway in MS. It is a reliable imaging technique with high repeatability. Retinal thickness loss was found in all MS subtypes and is associated with both physical and cognitive dysfunction. Our findings suggest the usefulness of measuring pRNFL thickness with OCT in MS eyes. In particular, the T-pRNFL thickness might be an important measurement to differentiate MS subtypes.

Keywords: Optical coherence tomography, Multiple sclerosis, Peripapillary retinal nerve fiber layer, Ganglion cell – inner plexiform layer, Physical disability, Cognitive impairment

LIST OF SCIENTIFIC PAPERS

I. Brautaset, R., **Birkeldh, U.**, Frehr Alstig, P., Wikén, P., Nilsson, M. Repeatability using automatic tracing with Canon OCT- HS100 and Zeiss Cirrus HD-OCT 5000. PLoS One. 2016;11(2):e0149138.

II. **Birkeldh, U.**, Manouchehrinia, A., Hietala, M.A., Hillert, J., Olsson, T., Piehl, F., Skelton Kockum, I., Brundin, L., Zahavi, O., Wahlberg Ramsay, M., Brautaset, R., Nilsson, M. Retinal nerve fiber layer thickness associates with cognitive impairment and physical disability in multiple sclerosis. Submitted for publication.

III. **Birkeldh, U.**, Manouchehrinia, A., Hietala, M.A., Hillert, J., Olsson, T., Piehl, F., Skelton Kockum, I., Brundin, L., Zahavi, O., Wahlberg Ramsay, M., Brautaset, R., Nilsson, M. The temporal retinal nerve fiber layer thickness is the most important optical coherence tomography estimate in multiple sclerosis. Frontiers in neurology. 2017;8:675.

LIST OF ADDITIONAL SCIENTIFIC PAPERS

Jansson, U., Brautaset, R., Cerviño, A., Nilsson, M. A comparison of the Canon TX-20P™ non-contact tonometer and pachymeter in healthy eyes. International journal of ophthalmic practice. 2012;3(3): 96-102.

Brautaset, R., **Birkeldh, U.**, Rosén, R., Wahlberg Ramsay, M., Nilsson, M. Reproducibility of disc and macula optical coherence tomography using the Canon OCT-HS100 as compared with the Zeiss Cirrus HD-OCT. European journal of ophthalmology. 2014; 24(5): 722-7.

Domínguez Vicent, A., **Birkeldh, U.**, Laurell, C.G., Nilsson, M., Brautaset, R. Objective assessment of nuclear and cortical cataracts through scheimpflug images: Agreement with the LOCS III scale. PLoS One. 2016;11(2):e0149249.

CONTENTS

LIST OF ABBREVIATIONS

DMT	Disease Modifying Treatment
EDSS	Expanded Disability Status Scale
GCC	Ganglion Cell Complex
GCIP	Ganglion Cell – Inner Plexiform Layer
HCs	Healthy Controls
MRI	Magnetic Resonance Imaging
mRNFL	Macular Retinal Nerve Fiber Layer
MS	Multiple Sclerosis
MSIS-29	Multiple Sclerosis Impact Scale 29
OCT	Optical Coherence Tomography
ON	Optic Neuritis
pRNFL	Peripapillary Retinal Nerve Fiber Layer
SDMT	Symbol Digit Modalities Test
SD-OCT	Spectral Domain Optical Coherence Tomography
SS-OCT	Swept Source Optical Coherence Tomography
TD-OCT	Time Domain Optical Coherence Tomography
T-pRNFL	Temporal Peripapillary Retinal Nerve Fiber Layer

1 PREFACE

During my master's studies I worked on a project about evaluating a certain electrode's capability to directly measure electrical activity of the ciliary muscle during accommodation. The aim was also to investigate if accommodation triggers electrical activity in several muscles of the neck and upper back and if this would correlate with the ciliary muscle activity. While working on the project I found myself very interested in research. After the master's program I got the opportunity to apply for a doctoral project. The main purpose of the project was initially to evaluate different techniques for the measurements of structure and function of the eye. My supervisor had an idea to evaluate ocular structure and function in patients with multiple sclerosis (MS) and during a division visit by the head of department this idea was again brought up. The head of department immediately got interested and promised to engage himself in this idea being realized. So more or less unexpectedly, our research group changed its focus and became involved in MS research focusing on optical coherence tomography (OCT). OCT in MS had only been done sparsely in Sweden and international studies showed positive results of using OCT in MS. So, from that day my project took another direction, i.e., towards structural retinal measurements.

2 INTRODUCTION

Medical imaging technologies have advanced dramatically over the last decade. Imaging is now essential to improve diagnosis accuracy and to create a good foundation to aid therapeutic decisions and future follow ups. New techniques do not only need to be compared with already established instruments, the repeatability must also be evaluated. Today the magnetic resonance imaging (MRI) is the most important tool for neurological conditions. MRI is a non-invasive technique; however it is also time consuming, expensive and uncomfortable for the patient (1). The ideal methods for monitoring axonal damage will be specific, inexpensive and can be performed quickly and frequently. These ideal methods should also monitor disease progression and response to therapy.

In many diseases, such as MS, an early diagnosis and the possibility for accurate quantitative measures of disease progress are crucial for clinical decision making and the patient's well-being. The retina is a unique central nervous system (CNS) structure with its unmyelinated ganglion cell axons, making it possible to image the axons directly. The back of the eye can be considered as the front of the brain, and already in 1974 Frisén et al. observed defects of the peripapillary retinal nerve fiber layer (pRNFL) in MS patients using ophthalmoscopy (2). By quantifying the RNFL and macular thickness, it might be possible to monitor axonal and neuronal damage (3). It is also important to investigate if structural changes correlate with disability. The afferent visual pathway is easy to investigate both structurally and functionally. Retinal tissue imaging is easily performed using OCT. This non-invasive technique has revolutionized the ophthalmology field and is nowadays a very important imaging tool when diagnosing several eye conditions.

2.1 AIMS OF THE THESIS

This thesis consists of three studies and the purpose was to investigate the potentials of OCT to assess retinal degeneration in patients with MS. The specific aim of each study was:

Paper 1: To investigate the repeatability of optic disc and macular measurements in healthy eyes obtained from Canon OCT-HS100 when using automatic tracing.

Paper 2: To assess the potential of measuring pRNFL thickness with OCT in MS eyes, both with and without optic neuritis history, and correlate it with commonly used functional tests in the MS field.

Paper 3: To compare different OCT parameters between MS patients and healthy controls and to investigate these parameters as predictive values for future physical disability and cognitive impairment in MS.

3 BACKGROUND

The first part of the background section of this thesis provides some basic concepts regarding the structure and function of the retina and visual pathway. Next, this background chapter focuses on the history and technology of OCT and how it has evolved since it was introduced a quarter of a decade ago. Thereafter, a section about MS with its impact on vision and close relationship to optic neuritis (ON) will follow. The last part of this chapter will give the reader the basic concepts about commonly used assessment scales in clinical practice and treatment trials for MS.

3.1 THE RETINA

The retina lines the back of the eye with a total diameter of 30-40 mm (4) and is composed of several different layers (Figure 1). Even though the retina contains many millions of neurons, there are only five different types of neurons in the retina.

The retinal pigment epithelium (RPE) is a single sheet of polygonal, melanin-containing cells situated on the Bruch's membrane. The photoreceptors are in connection with the RPE layer and consists of an inner and an outer segment (IS/OS). The external limiting membrane (ELM) has intercellular junctions and divides the inner segment of the photoreceptor from its cell body and synaptic terminal. The outer nuclear layer (ONL) contains the cell bodies of the photoreceptors. The outer plexiform layer (OPL) is the first synaptic zone and consists of synapses connecting the photoreceptors to the horizontal cells and the bipolar cells. The inner nuclear layer (INL) contains the cell bodies of horizontal cells, bipolar cells, amacrine cells and Müller cells. The bipolar cells terminate on the amacrine cells and ganglion cells in the inner plexiform layer (IPL), which is the second synaptic zone of the retina. The ganglion cell layer (GCL) contains the cell bodies of the ganglion cells. The RNFL is composed of the ganglion cell axons which form the optic nerve. The inner limiting membrane (ILM) is the basement membrane of the Müller cells and represents the border between the retina and the vitreous body (5).

Vision is initiated by phototransduction, a process when light is converted into an electrical signal by the photoreceptors. The photoreceptors outer segment contains the light sensitive visual pigment rhodopsin. When light is absorbed by rhodopsin a receptor potential will trigger a chain of events that amplifies the electrical signal to the rest of the photoreceptor (6, 7).

The visual information arising in the photoreceptors travel through the bipolar cells to the ganglion cells. The photoreceptors consist of rods and cones. The rods have very low spatial resolution but are extremely sensitive to light and are responsible to low-light vision. Cones, on the other hand, have high resolution, but are insensitive to light and mediate daylight vision and color vision (8). The bipolar cells connect the outer and the inner retina and these cells contact every other retinal neuron type (9). They receive electrical impulses directly from the photoreceptors or indirectly from the horizontal cells and carries the information to the IPL where they synapse on ganglion cells. More than ten types of bipolar cells are present

in the retina. The horizontal cells are spread horizontally in the INL and regulate the input from photoreceptors to bipolar cells (10, 11). Amacrine cells have the highest variety of all cells in the retina and 30 different types have been identified. They have an inhibitory nature and stand in connection with bipolar and/or ganglion cells (12).

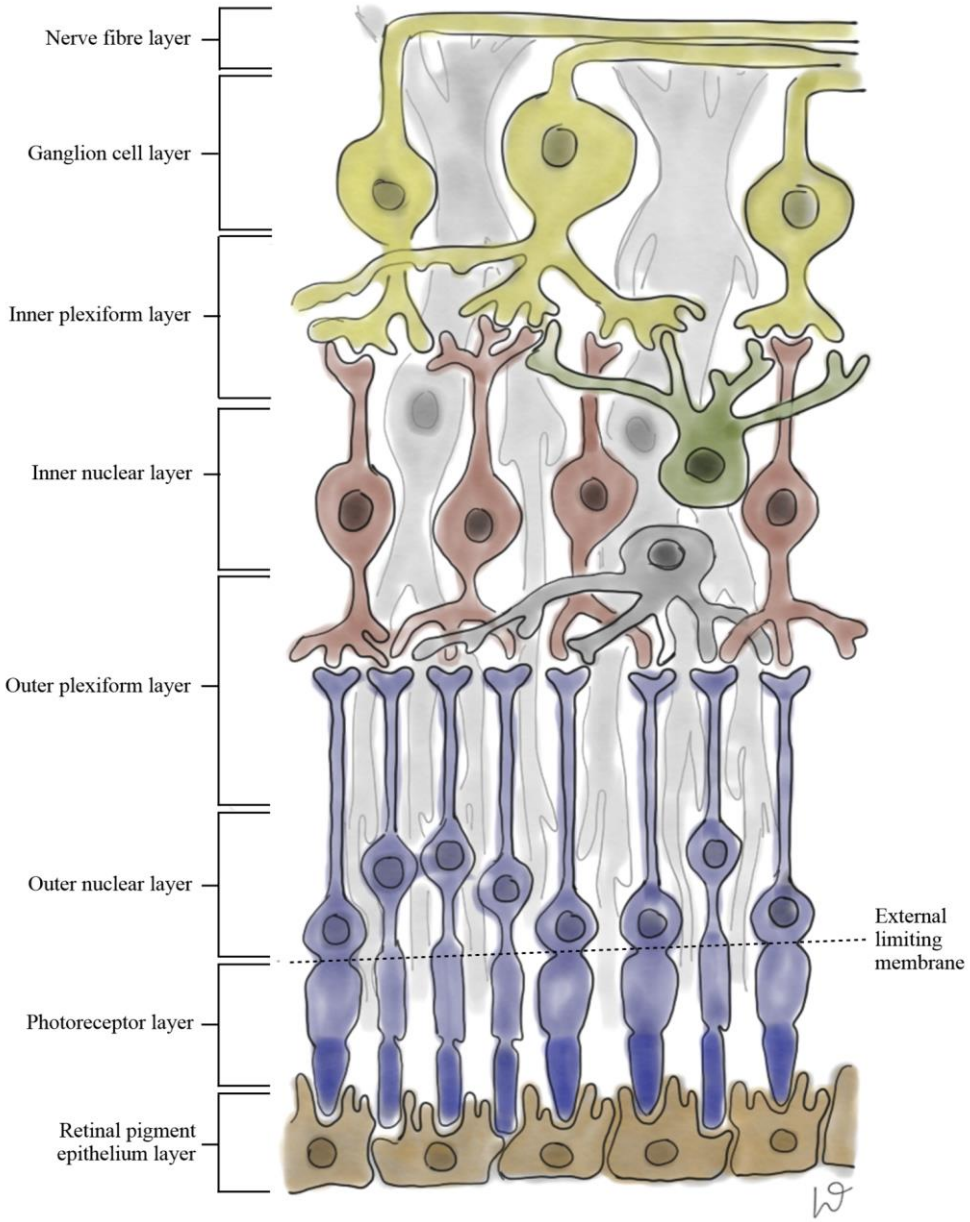

Figure 1. Illustration by L. Pettersson of the retinal layers. The illustration is printed with permission from the illustrator and is modified from Hansen (13).

3.2 VISUAL PATHWAY

The ganglion cell axons exit the retina through the optic disc and form the optic nerve. The optic nerve axons travel to the optic chiasm where most axons will undergo a partial decussation and afterwards enter one of the two optic tracts. The optic tracts consist of axons from both eyes and most of them will terminate in the lateral geniculate nucleus, the thalamic relay nucleus for vision (5). The lateral geniculate nucleus both separates the input from each eye into different layers and from different types of ganglion cells. The main types of

ganglion cells are the parvocellular neurons (midget cells) and the magnocellular neurons (parasol cells). The small parvocellular neurons, mostly found in the fovea, detects fine details and are responsible for the "what"-pathway, are sensitive to color and form (5, 8). The magnocellular ganglion cells, which are predominant in the peripheral retina, have larger cell bodies and axons than the parvocellular neurons and are concerned with the "where"-pathway. They are "color blind", detects motion and have high-contrast sensitivity (8, 14).

The internal capsule contains many projecting fibers and is divided in five different regions. The retrolenticular region of the internal capsule contains the optic radiation. The axons of the optic radiation, originating in the lateral geniculate nucleus, consist of three fiber bundles and they terminate in the calcarine sulcus of the occipital cortex (8). The axons of the optic radiation give rise to a retinotopic map. The ventral/anterior bundle, called the Meyer's loop, are the axons representing the inferior retinal quadrants, that give rise to the superior visual field quadrants. These axons loop deeply into the anterior temporal lobe before taking a turn backwards to the anteroinferior portion of the calcarine sulcus (15, 16). The central bundle occupies a large middle area of the optic radiation fibers and corresponds to the macular region, i.e. the central visual field (5). The dorsal/posterior bundle, the Baum's loop, are the axons representing the superior retinal quadrants, that give rise to the inferior visual field quadrants. These axons projects superiorly towards the occipital cortex through the parietal lobe (17). An overview of the visual pathway is illustrated in Figure 2.

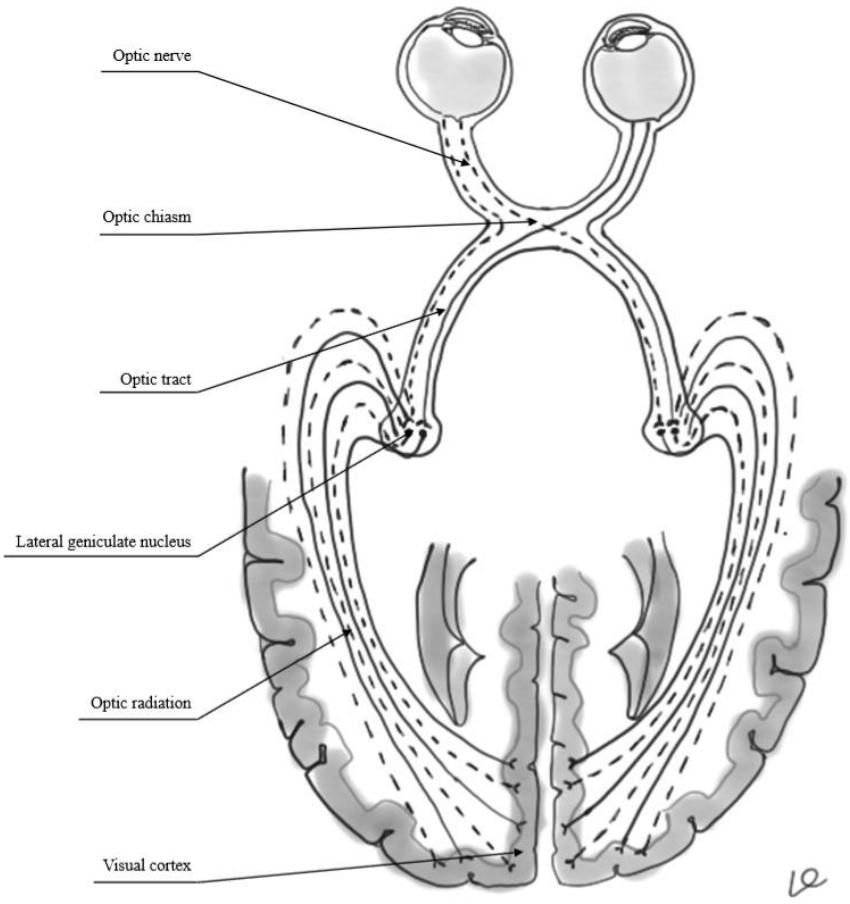

Figure 2. Illustration of the visual pathway from the retina to the primary visual cortex by L. Pettersson. The illustration is printed with permission from the illustrator and is modified from Hansen (13).

3.3 OPTICAL COHERENCE TOMOGRAPHY

3.3.1 History

Optical coherence tomography (OCT) was first described in 1991 by Huang et al. as a non-invasive imaging technique for evaluation of biological systems in vitro (18). Two years later the technique was presented as an in vivo imaging of healthy human retinas (19, 20). A few years later imaging of several macular diseases was performed for the first time with OCT (21). The technique has since then become an accepted and powerful diagnostic tool for retinal pathologies and reveals a potential decrease in RNFL and macular thickness (22, 23). Today it is used for evaluation and follow-up of several retinal conditions and diseases, such as macular holes (24), epiretinal membranes (25), macular edema (26) and glaucoma (27). The images obtained are very similar to histologic sections and the technique might be considered as in vivo histology (23).

3.3.2 Basic principles of the technique

The principle technique of OCT uses light waves to take cross-sectional images of retinal tissue structure in real time. It is based on an echo technique and the principle is almost the same as ultrasound imaging, but instead of using sound, it uses light. The OCT images have higher resolution compared with ultrasound or radiofrequency. It uses a low-coherent, super luminescent diode of near-infrared light (approximately 840 nm), which is divided by a beam-splitter into a reference beam and a detection beam (18). The reference beam goes to a reference mirror and the detection beam goes to the eye. The reference beam is then reflected by its mirror and the detection beam is backscattered with different time delays by the retinal tissue. The beams are then recombined through the beam splitter, detected by a photo detector and an image is obtained by comparing the time difference in the backscattered light from the different retinal layers with the light reference reflection. The intensity of backscattered light at different retinal depths at a single location will provide structural information, known as A-scans. Combining multiple A-scans gives two-dimensional images, called B-scans.

Time-domain OCT (TD-OCT), the old generation of OCT, uses a moving reference mirror which gives a very slow scanning speed. The commercially available TD-OCT Stratus OCT (Carl Zeiss Meditec, Dublin, CA) produces 400 A-scans per second with an axial resolution of 8-10 µm. However, the newer technique, spectral-domain OCT (SD-OCT), uses a fixed reference mirror and the photo detector is replaced by a spectrometer (28). This makes the scanning speed much faster with at least 25,000 A-scans per second and three-dimensional images are obtained (29). The axial resolution is 3-6 µm. In comparison with TD-OCT, it is possible to quantify the different retinal layers individually with the technology of SD-OCT. In 2012, Canon launched the SD-OCT HS100 (Figure 3). The scan speed is 70,000 A-scans per second, which enables a short examination time. The axial resolution is 3 µm. The scanning width varies between 2 and 10 mm, depending on type of scan. The Canon OCT-HS100 is further described in the Methods section.

The latest generation of OCT, swept source OCT (SS-OCT), has recently been introduced. In SS-OCT, the super luminescent diode is replaced by a tunable, short cavity swept laser and a spectrometer is not used (30). The laser changes in each scan when it sweeps across a band of wavelengths and the median wavelength in SS-OCT is 1,050 nm (31). This enables not only a scanning speed of 100,000 A-scans per second, but also improved image quality since it penetrates the tissue deeper and visualizes the choroidal structures. These features are advantageous when studying the vasculature of the retina and choroid with OCT angiography (30). This is a novel non-invasive technique that visualizes the vessels by detecting flowing red blood cells (32).

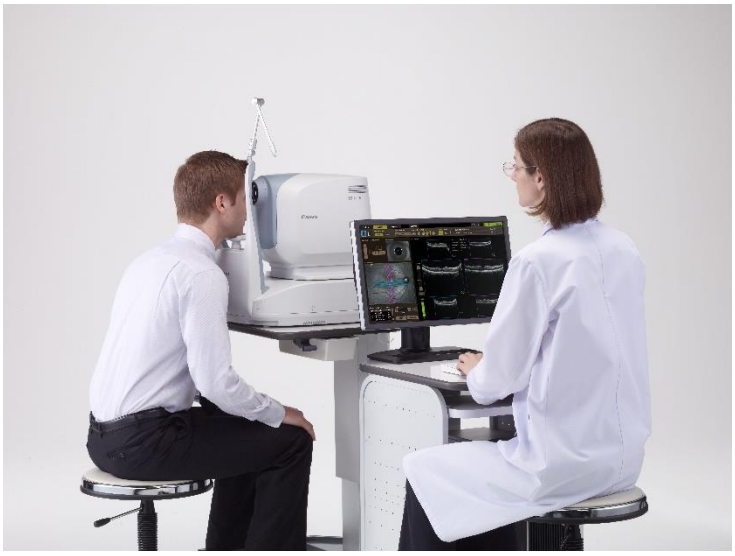

Figure 3. Image of patient being measured with Canon OCT-HS100. Image published with permission from Canon Europe, Amstelveen, Netherlands.

3.3.3 Retinal images obtained with OCT

With the technology of SD-OCT, and its improved axial resolution, it is now possible to investigate the different layers individually. This is done with intraretinal segmentation algorithms which now are incorporated into the software and is performed automatically. Before the time of segmentation algorithms, the retinal ganglion cell thickness was studied as a total macular volume and not as an individual layer (33). The OCTs of today only requires pupil dilation if the pupil diameter is less than 3 mm. Since OCT is depending on optical properties of the eye, ocular media opacities, such as cataract or vitreous body opacity, are factors that might decrease the signal strength, i.e. loss of image quality (23)

OCT images are presented either in gray scale (Figure 4) or in color. The more hyper reflecting layers will appear brighter than the hypo reflecting layers on the gray scale image and different colors will correspond to different degrees of tissue reflectivity on the colored image (23). The axonal containing layers, macular RNFL (mRNFL), IPL and OPL, backscatters more light than the nuclear layers GCL, INL and ONL and therefore appear more hyper reflecting on SD-OCT images (34). Two highly reflective and distinctive layers of the outer retina seen in an SD-OCT scan are the ELM and the RPE (35).

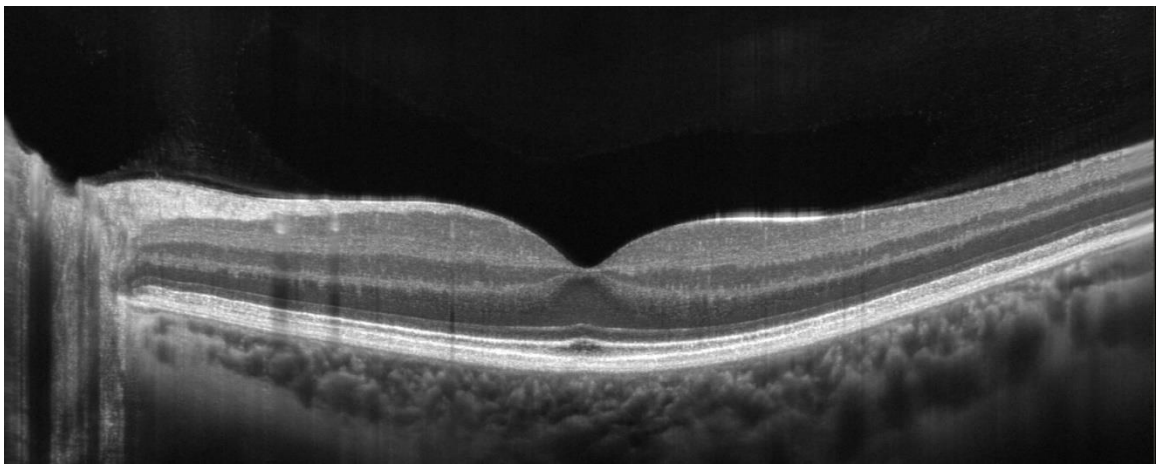

Figure 4. SD-OCT scan of a normal left eye displayed in gray scale, showing the vitreous, retinal layers and choroid. The image was obtained by U. Birkeldh with Canon OCT-HS100.

3.4 MULTIPLE SCLEROSIS

3.4.1 An overview of the disease

MS is a chronic inflammation of the CNS which aims for both gray and white matter (36). It affects about 2.5 million individuals worldwide and is the leading cause of non-traumatic disability in young adults (37-39). The incidence of MS peaks around 30 years of age (40). The overall prevalence in Europe is 83 per 100,000 inhabitants (41). The prevalence in Sweden is ~189 per 100,000 inhabitants and is one of the highest in the world (42). There is a female preponderance in MS and the female to male ratio reported in Sweden is 2.35:1 (42). The etiology is unknown. Both genetic and environmental factors have been proposed to play a role in the disease development and progression (38, 43). It is believed that MS outbreak derives from interactions between environment and genetics (44). Environmental risk factors other than latitude associated with MS are vitamin D status, obesity in childhood, smoking and infections (45). Even though MS is not considered to be hereditary there are some genetic factors that are known to have a close relationship to MS and might increase the risk of disease development (39). About 20% of all MS patients have a relative with the disease and the hereditary factor that has been found to have the highest association with MS is the human leukocyte antigen (HLA) complex (41, 46). The HLA gene complex on chromosome 6 is associated with the immune system and this is supporting the theory of MS as an autoimmune disease (47, 48).

The blood-brain barrier (BBB) plays an important role in MS and the disease is thought to begin with disruption of the BBB due to acute inflammatory lesions (48). It has been found that the BBB might present higher permeability in normal appearing white matter in MS patients compared to healthy controls (HCs). This increased passage of leukocytes into the CNS leads to demyelination and axonal loss (49). MS is classically thought of as a demyelinating disease, but it is also known that the pathology is much more complex. The isolating myelin covers of the nerve cells are damaged and become edematous and consequently expands the axon diameter in the brain as well as in the spinal cord (50).

The chronic disability seen in MS is mainly due to neuro-axonal degeneration rather than demyelination (51) and this process seem to occur early in the disease course (52). This damage disrupts the communication between cells in the CNS which produces a wide range of symptoms.

Depending on where the lesions are located within the CNS, the symptoms may vary among the MS patients (53). The symptoms can include cognitive impairment (such as deficits in attention, information-processing speed and impaired memory), changes in sensation (numbness and tingling in one or more limbs), muscle weakness, chronic pain, spasms, tremor, depression, Lhermitte's sign (electrical sensation that runs down the spine triggered by flexing the head forward) and fatigue among others (38). The overall prevalence of cognitive dysfunction in MS has shown to be over 40% and 37% of the cognitively preserved MS patients have been reported to develop cognitive dysfunction after four years (54). Vision loss is a common first manifestation of MS and is caused by ON. MS might also debut with internuclear ophthalmoplegia, which is characterized with impaired eye movements, such as diplopia and nystagmus (38). This is due to a lesion involving the medial longitudinal fasciculus in the brainstem (55). Uhthoff's phenomenon is when the symptoms are worsened due to increased body temperature (after exercise or a hot bath) and is common among MS patients (56). Approximately 30% of all MS patients experience persistent visual disturbances, such as visual fatigue, blurred vision, diplopia and visual instability, despite wearing glasses. These complaints were not related to a recent MS relapse (57).

There is no known cure for MS, but there are several treatments. The medications focus on slowing disease progression, decrease frequency and severity of relapses and MS related symptoms (41). Rehabilitation programs might be a complement to the pharmacological treatment and aim to maintain and improve the general health of MS patients (58). Life expectancy is 5 to 10 years shorter than that of an unaffected population (53). The diagnosis of MS may take many years. There is an international consensus for the use of specific criteria that include typical MS lesions in the CNS disseminated in space and time and in a combination with the patient's symptoms or relapses. These revised McDonald criteria from 2010 are based to a greater extent than before on the MRI findings. This makes it possible in some cases to speed the diagnostic process (59). MRI is the gold standard imaging tool for brain atrophy in MS. Brain atrophy seen in MS patients has been shown to predict cognitive impairment (60).

3.4.2 Disease subtypes

A clinically isolated syndrome (CIS) is the first clinical deficit suggestive of MS (61). A relapse of MS is an acute inflammatory event in the CNS that leads to a neurological symptom in the absence of an infection or fever and persists for at least 24 hours (41, 62). About 85% of the patients are initially diagnosed with the disease course of relapsing remitting MS (RRMS) (62, 63). This non-progressive type is characterized with relapses that may last from a few days to several weeks and are followed by full or partial recovery (64). Years after onset many of initially RRMS patients often converts into secondary progressive

MS (SPMS) with an increase in disability because of poor functional recovery (41). About 10-15% of the patients are diagnosed with a primary progressive form of MS (PPMS) at the time of disease onset. PPMS is characterized with an on-going accumulation of functional disability, especially associated with lesions in the spinal cord, without any typical relapses from the very beginning of the disease (63, 65). PPMS has an incidence that is similar among males and females. The different subtypes are presented in Figure 5.

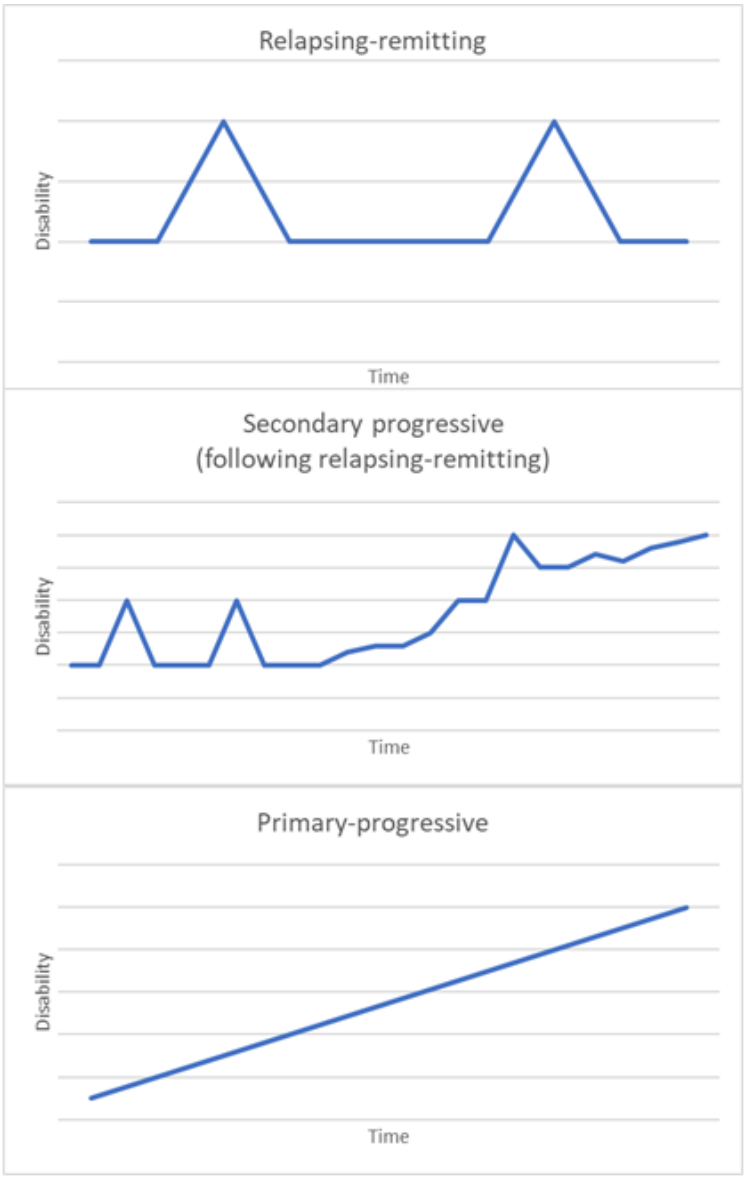

Figure 5. A graph illustrating the different subtypes of multiple sclerosis with inspiration from Hillert et al. (66). Illustration: U. Birkeldh.

3.4.3 Optic neuritis

ON has a close relationship to MS and is the first manifestation in 25% of all cases and 70% of all patients will at some point during the illness experience an episode of ON (67). Approximately 50% of all patients with ON will develop MS within 15 years after ON onset (68). It is a demyelinating inflammation of the optic nerve and is usually unilateral.

Sometimes abnormalities of the optic nerve are found in the absence of ocular symptoms in MS patients. This structural change might be explained by subtle subclinical events of ON that does not result in clinically obvious ON (69). The typical symptoms patients report is reduced visual acuity, retrobulbar pain especially during eye movements, dyschromatopsia and reduced contrast sensitivity (70, 71). The vision loss might span from mild to severe and progresses the first 1-2 weeks after onset (70). Important clinical signs are relative afferent pupillary defect and visual loss, usually with a central scotoma (72).

ON is divided into retrobulbar neuritis and the less common papillitis (67). Retrobulbar neuritis is an inflammation of the optic nerve behind the globe and therefore initially the fundus exam appears normal. Papillitis presents with swelling of the optic disc due to the intraocular inflammation (72). Optic disc pallor usually develops 4-6 weeks after ON onset. Also, an initial quick recovery begins at this timepoint followed by a slower process and the final visual improvement might not be stabilized until one year after onset (73, 74). A statistically significant decrease in pRNFL thickness after ON compared with the unaffected fellow eye has been shown even in patients who demonstrated good visual recovery. However, a larger pRNFL loss correlates with less complete visual function recovery (75). High-contrast visual acuity testing is considered an insensitive functional test in ON compared to other measures (75-77). It has been found that MS patients with normal high-contrast visual acuity have reduced pRNFL thickness compared to HCs. However, in the same MS patient cohort it was found that this loss of pRNFL thickness correlates well with reduced scores in low-contrast visual acuity (76). Gabilondo et al. demonstrated that a loss of ≥ 4.5 μm in the ganglion cell-inner plexiform layer (GCIP) one month after ON onset predicts poor recovery of low-contrast visual acuity six months after onset (78).

3.5 THE UTILITY OF OCT IN MS

The usefulness of OCT in MS has been discussed for more than a decade. It is still unknown whether any of the retinal layers is superior to the others when distinguishing MS patients from HCs. Early MS-OCT studies used TD-OCT and reported thinning of pRNFL thickness and/or macular volume loss compared with HCs (76, 79, 80). Petzold et al. have reported two comprehensive meta-analyzes regarding retinal layer quantification using OCT (3, 81), the first with TD-OCT and the recently published paper included only SD-OCT. The pRNFL data found for the SD-OCT was very similar to the previous TD-OCT data. This finding accentuates the pRNFL as a precise measure for measuring the neurodegeneration in MS. In the SD-OCT meta-analysis they also reported atrophy of the mRNFL and GCIP, but no atrophy was found in the INL (81). A large histopathological study with 82 MS patients, by Green et al., found that INL atrophy was only found in eyes of patients who had longstanding disease and that INL atrophy was associated with the severity of GCIP loss (82). Microcystic macular edema, measured with OCT, has been found in MS patients with ON history and it was mostly seen in the INL (83). Retinal inflammation, which might be the underlying cause of the INL thickness increase, has been found in MS patients with more active disease activity (80, 81).

It has been suggested that thinning of the retinal layers begin early in the disease (52). Atrophy of the retinal layers found with OCT in patients without previous ON could be explained either by subclinical ON that might have gone unnoticed or by primary retinal pathology related to MS (84). Another suggested explanation for retinal atrophy without ON history is retrograde trans-synaptic degeneration (84-86). This is a process when neuronal damage is spread backwards through the synapses from a sick neuron to a healthy neuron. Klistorner et al. reported that the optic radiations, measured with MRI, are often injured in MS patients without ON history and pRNFL thickness, measured with OCT, is significantly reduced in these eyes (87). Several other studies have also shown a correlation between different MRI brain atrophy markers and OCT parameters of retinal degeneration the past ten years (88-92). Saidha et al. reported a 4-year follow-up study of MS patients with significant correlations between GCIP loss and the MRI parameters whole brain atrophy, gray matter, white matter and thalamic regions (88). These findings suggest that OCT parameters and MS related brain atrophy are linked and therefore OCT measurements might be valuable in this patient group.

3.6 ASSESSMENT SCALES IN MS

3.6.1 Expanded disability status scale

The expanded disability status scale (EDSS) is the most commonly used assessment scale for quantifying neurological disability in MS. It was developed by the neurologist John Kurtzke in 1983 and is a revision of his previous disability status scale from 1955 (93). EDSS quantifies the disability in MS in eight functional systems: Pyramidal, cerebellar, brain stem, sensory, bowel & bladder, visual, cerebral and other functions. Each functional system is assigned with a score on a scale that ranges from 0 to 10 in half points. The higher the number is, the greater the disability is (0 = no disability, 10 = death due to MS) (93). Just by looking at the EDSS score the examiner gets a rough idea of the function level of the patient. EDSS score 4.0 indicates maximum walking distance of 500m. EDSS score higher than 4.5 are defined by the impairment to walking. EDSS has been criticized for its high inter-rater variability and for mostly emphasizing the walking ability and barely evaluating the arms or cognitive dysfunction.

3.6.2 Symbol digit modalities test

The symbol digit modalities test (SDMT) is a screening test for cerebral dysfunction in both children and adults. It is based on neuropsychological principles and is very simple to perform and administrate (94). SDMT is widely used for screening cognitive impairment in patients with MS (95, 96). SDMT measures information processing speed and it takes approximately 5 minutes to perform (97). The task is based on the conversion of randomized geometric figures into numbers. The correct number corresponding to a specific figure is presented for the patient in a key containing the numbers 1 to 9. The test can be performed either written or oral to overcome different physical dysfunctions, such as motor handicaps or speech disorders (94).

3.6.3 Multiple sclerosis impact scale 29

Self-report scales are frequently used measures of MS and give the patients' perspective of the disease. The multiple sclerosis impact scale (MSIS-29) was developed in 2001 and is commonly used (98). This patient-based rating scale consists of 29 questions of which 20 concerns the physical impact and nine the psychological impact of MS. Each question has five options where the patient grades the impact of MS in his/her daily life (1 = not at all; 5 = extremely). The score for physical and psychological can be presented both separately and as a combined score.

4 MATERIALS AND METHODS

4.1 MATERIAL/DATA COLLECTION

In paper I subjects were recruited in the outpatient clinic at the Unit of Optometry, St. Erik Eye Hospital, Stockholm. Only subjects without any ocular pathology were included in the study. Exclusion criteria were history or evidence of macular disease, neurologic disease, glaucoma, media opacities, poor OCT image quality and a history of ocular trauma. Only the right eye of each subject was included. Thirty subjects (mean age 35.3 years, range 22-66 years, female/male ratio 24/6) were enrolled.

In paper II and III the MS patients were recruited when coming to their annual routine examination (Paper II: May 2013-October 2015; Paper III: May 2013-May 2016) at the Neurology Clinic, Neuro Centrum, Karolinska University Hospital, Solna. A total of 465 MS patients were enrolled in paper II and 546 MS patients participated in paper III. All included patients had a diagnosis of RRMS, SPMS or PPMS. They were excluded if they had an episode of ON during the last 6 months, other neurological disorders or ocular diseases that might influence the outcome measures. Disease duration, treatments and ON history were recorded. ON history was confirmed from medical records or by patient self-reports.

In paper II and III a group of HCs were enrolled to age and sex match the MS group. The HCs consisted of both subjects from Paper I, staff at St. Erik Eye Hospital, optometry students and their family members. The same inclusion and exclusion criteria from paper I were used. One hundred sixty-eight healthy subjects (42.3 ± 15.4 years, female/male ratio 129/39) were enrolled in paper II and one hundred seventy-five healthy subjects (42.5 years ± 15.4, female/male ratio 134/41) in paper III. All HCs underwent an ophthalmologic examination prior to inclusion.

4.2 METHODS

Paper I was designed to evaluate the test-retest reliability for the Canon OCT-HS100 and Zeiss Cirrus HD-OCT 5000 in healthy subjects, using the new automatic eye tracking function. The Canon OCT-HS100 with software version 4.0 (Canon Europe, Amstelveen, Netherlands), which performs up to 70,000 A-scans per second with an axial resolution of 3 µm. It has a scanning depth of 2 mm. The scan mode "Disc 3D" was used to analyze optic nerve head and the surrounding pRNFL, see Figure 6. It measures an area of 6x6 mm with 256 B-scans each consisting of 512 A-scans. The scan diameter circle is 3.45 mm centering on the optic disc. The macular measurements were performed within a 10x10 mm area using the "Macula 3D" scan mode, which has 128 B-scans, each consisting of 1,024 A-scans. The Cirrus HD-OCT 5000 (Carl Zeiss Meditec, Inc., Dublin, California, USA) has an A-scan velocity of 27,000 scans per second with an axial resolution of 5 µm and scanning depth of 2 mm. The optic nerve head and pRNFL measurements were performed with scan mode "Optic Disc Cube", which acquires 200 B-scans, each composed of 200 A-scans. The scan circle has a diameter of 3.46 mm and is centered on the optic disc. Measurements of the macular area were obtained with "Macular Cube" which has a scan pattern of 128 B-scans,

each composed of 512 A-scans. Both “Optic Disc Cube” and “Macular Cube” measures within a 6x6 mm area.

Each subject was measured twice with each OCT, without the use of mydriatic drops, within one hour and re-seated before the second scan. One OCT operator was responsible for the Canon (P.F.A.) and one for the Zeiss instrument (U.B.).

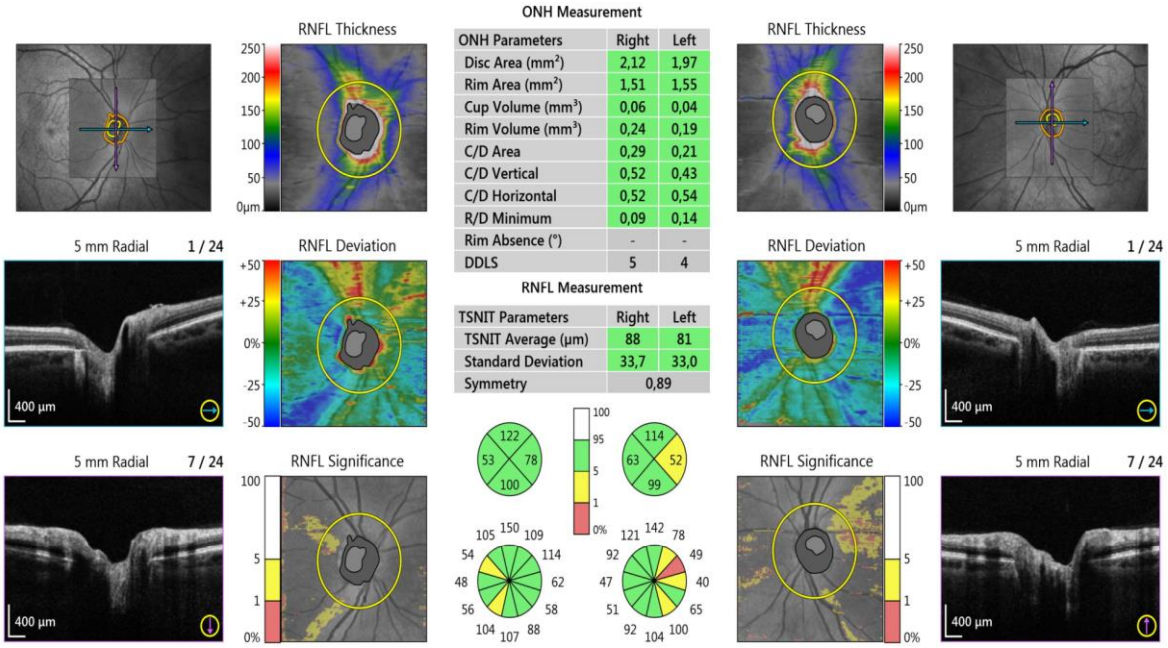

Figure 6. The report view of “Disc 3D” with the optic disc parameters. Image obtained by U. Birkeldh with Canon OCT-HS100 (version 4.00).

A total of nine optic disc parameters were analyzed for both instruments: Disc area, rim area, cup volume, vertical cup/disc ratio, pRNFL thickness in the four quadrants (inferior, superior, nasal and temporal) and the overall average pRNFL thickness 360° around the optic nerve head. For the macular measurements the thickness value in each of the nine subfields corresponding to the Early Treatment of Diabetic Retinopathy Study (ETDRS) were analyzed, see Figure 7.

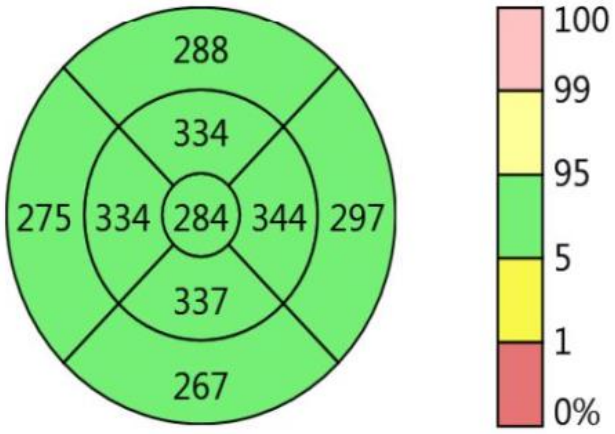

Figure 7. The nine subfields of macular thickness corresponding to the Early Treatment of Diabetic Retinopathy (EDTRS). Image obtained by U. Birkeldh from the report view of "Macula 3D" with Canon OCT-HS100.

Paper II was designed to cross-sectionally investigate the pRNFL thickness in all MS subtypes compared to HCs and to find possible correlations between pRNFL and different neurological clinical measures. SD-OCT measures were performed using the same Canon - HS100 with software version 4.0 from paper I. The scan mode "Disc 3D" was used for the pRNFL measurements in both MS patients and HCs. The thickness values analyzed were the four quadrants (inferior, superior, nasal and temporal) and the overall average value of the whole pRNFL 360° around the optic nerve head.

In paper III possible correlations between the average pRNFL, temporal RNFL (T-pRNFL), macular thickness and different clinical outcomes in MS patients were evaluated. Both "Disc 3D" and "Glaucoma 3D" were performed and with the same Canon OCT-HS100 (software version 4.2.0) as in paper I and II. The "Glaucoma 3D" was used for the measurements around the fovea and is composed of 128 B-scans each consisting of 1,024 A-scans. This macular scan mode measures the thickness over a 10x10 mm area which is centered on the fovea. The thickness map is composed of one inner ring (the area bounded by the central circle of 1.5 mm diameter and the middle circle of 5 mm diameter) and one outer ring (the area bounded by the middle circle of 5 mm diameter and the outer circle of 10 mm diameter), each with four subfields (Figure 8). For both the inner and outer ring, the thickness of macular retinal nerve fiber layer + macular ganglion cell layer + macular inner plexiform layer complex (GCC) is obtained. The GCIP thickness was also obtained from this thickness map. Segmentation of the retinal layers was acquired automatically using the incorporated segmentation software.

In paper II and III the physical disability was assessed with EDSS by an experienced neurologist. Cognitive impairment was assessed with SDMT by one of the MS nurses. MSIS-29 was used to measure the physical and psychological impact of MS from the patient's point of view. These measurements were collected from the Swedish MS register and performed during the patients' routine visit.

The measurements were obtained from both eyes in normal daylight conditions of each patient in a single session with the same device and replicated three times. Measurements were performed on both the MS group and HCs, primarily by the same examiner (U.B.). The pupils were not dilated before OCT measurements. All images were checked manually afterwards for artefacts and adequate signal strength ≥7 (maximum, 10). Further quality assessment was performed according to the OSCAR-1B criteria (99) and the Advised Protocol for OCT Study Terminology and Elements (APOSTEL) recommendations (100). The scan with the highest quality was included in the analysis.

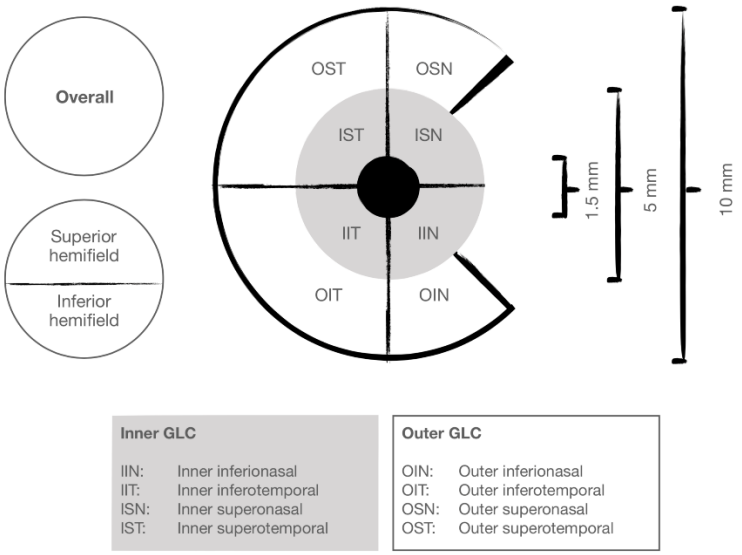

Figure 8: Illustration of the thickness map around the fovea in scan mode "Glaucoma 3D" with SD-OCT Canon HS100, inspired from Ng et al. (101). Printed with permission from the illustrator, L. Pettersson.

4.3 STATISTICS

In paper I the coefficient of repeatability (CR) for each of all optic disc and macular parameters was calculated according to the Bland-Altman method (102). The CR value was also calculated as a percentage of the mean (CR%). For each of all OCT parameters the squared Pearson correlation coefficient was calculated to determine the relationship between first and second measure. The statistical analysis used for the investigation of possible differences between the first and second measure was the one-sample t-test for normally distributed data. Wilcoxon rank-sum test was used for those measurements when the data was not normally distributed. The mean difference for each of all included OCT parameters between the two instruments were statistically compared with each other using a one-way ANOVA with Tukey post-hoc test. The two OCT's were also statistically compared according to their CR values with a paired t-test. All statistical analyzes were performed using Instat™ GraphPad Software Inc. version 3.

For paper II, the comparison of overall average pRNFL thickness and the pRNFL thickness in each quadrant (inferior, superior, nasal and temporal) between MS subtypes and HCs was performed using linear mixed effect models. These analyzes were accounting for within-patient inter-eye correlations and adjusted for age, sex and previous history of ON. The linear mixed effect models within MS were designed to assess the cross-sectional relationship between average pRNFL and pRNFL in the four quadrants and EDSS, SDMT and MSIS-29 (divided in physical and psychological scales). These models were adjusted for age, sex, ON history, disease duration, MS subtype and duration of exposure to first and second line disease modifying treatments (DMTs). All analyzes were performed using R version 3.3.2 (R Core Team, 2016) and package Non-Linear Mixed Effects.

In paper III, the thicknesses of overall average pRNFL, T-pRNFL, inner ring of GCC (inner GCC), outer ring of GCC (outer GCC), inner ring of GCIP (inner GCIP) and outer ring of GCIP (outer GCIP) were compared between MS including all subtypes, each MS subtype separately and HCs, using generalized estimation equation (GEE) models. The GEE models were designed to account for within-subject inter-eye correlations. These models were also corrected for age, sex and previous history of ON. For the comparison of MS only, the association between the different OCT measures and EDSS, SDMT and MSIS-29 (both physical and physiological) was analyzed using GEE models. These models were corrected for age, sex, previous ON history, disease duration, MS subtype and duration of exposure to DMTs. The number of previous SDMT examinations was taken into account as an additional adjustment in the model when the SDMT score was investigated. The analyzes regarding OCT measures and their relationship to EDSS, SDMT and MSIS-29 were also performed on eyes with no history of ON. This was done to make sure that the statistical correction for ON was sufficient enough since previous ON might be significantly different among individuals.

The predictive value of different baseline OCT measures on the trajectory of consecutive SDMT and EDSS scores was evaluated over a 36-month follow-up period. The evaluated measures in the longitudinal assessment were baseline average pRNFL, T-pRNFL, inner GCC and inner GCIP thicknesses. Measurements were categorized into two groups of "reduced" and "normal." "Normal" OCT measure was defined if the measurement was within one standard deviation of the respective measure in HCs. The OCT measure was considered "reduced" if the measurement was two or more standard deviations lower than the respective measure in HCs. GEE models were applied in the longitudinal analysis and corrected for age, sex, previous ON history, MS onset age, MS subtype and duration of exposure to DMTs. This was an exploratory analysis so that no correction for multiple comparisons was made. All analyzes were performed using R version 3.3.2 (R Core Team, 2016) and package geepack.

The significance threshold was set to $P < 0.05$ in all three studies in this thesis.

4.4 ETHICS

Informed consent was obtained from all participants prior inclusion. The studies were approved by the Regional Ethical Review Board in Stockholm (DNR 2009/2107-31/2 and 2011/874-31/2) and were performed according with the ethical standards stated in the Declaration of Helsinki.

5 RESULTS

5.1 PAPER I

5.1.1 OCT measures within instruments

The test-retest reliability was good for all analyzed parameters in both OCT's, according to the CR values. The CR% for the optic disc measurements ranged between 0.90% and 22.22% and between 0.00% and 16.00% with Canon OCT-HS100 and Zeiss Cirrus HD-OCT 5000 respectively. Both instruments showed high correlations between the two measurements in each of all included parameters, the R^2 value ranging from 0.76 to 0.98 for Canon and from 0.94 to 0.99 with Zeiss. No statistical difference was found between the two measurements for any of the parameters in both instruments ($p > 0.05$). The optic disc measurements within each OCT are presented in Table 1.

Table 1. Repeatability of optic disc parameters.

	Canon OCT-HS100					**Zeiss Cirrus HD-OCT 5000**				
	Mean	**CR**	**CR%**	**R^2**	**p**	**Mean**	**CR**	**CR%**	**R^2**	**p**
Disc area (mm^2)	2.08 ± 0.41	0.21	10.10	0.92	0.61	1.87 ± 0.35	0.10	5.34	0.96	0.71
Rim area (mm^2)	1.58 ± 0.37	0.20	12.66	0.97	0.55	1.41 ± 0.24	0.08	5.67	0.97	0.97
Cup volume (mm^3)	0.09 ± 0.12	0.02	22.22	0.98	0.63	0.13 ± 0.12	0.02	16.00	0.99	0.71
Cup/Disc vertical ratio	0.48 ± 0.14	0.05	10.41	0.97	0.99	0.47 ± 0.12	0.04	8.51	0.96	0.45
RNFL average (µm)	99.16 ± 8.57	5.46	5.51	0.93	0.15	93.96 ± 8.95	3.39	3.61	0.96	0.21
RNFL Inferior (µm)	127.80 ± 36.47	1.15	0.90	0.92	0.71	122.86 ± 34.41	1.09	0.89	0.96	0.61
RNFL Superior (µm)	118.36 ± 31.43	2.27	1.92	0.76	0.16	112.57 ± 30.29	0.89	0.79	0.94	0.68
RNFL Nasal (µm)	80.52 ± 18.94	2.09	2.60	0.89	0.15	72.23 ± 17.33	0.00	0	0.98	0.99
RNFL Temporal (µm)	69.60 ± 16.03	1.50	2.16	0.91	0.35	65.11 ± 16.24	0.89	1.37	0.97	0.53

RNFL = retinal nerve fiber layer, CR = coefficient of repeatability; CR% = coefficient of repeatability as a percentage of mean

The CR% for the macular measurements were lower than in the optic disc, i.e. the repeatability was better in the macula. The values ranged from 0.62 to 2.81% for Canon and 0.99 to 1.81% for Zeiss. The R^2 for the macular region was high and ranged between 0.89 and 0.99 and 0.93-0.99 with Canon and Zeiss respectively. There was no statistical difference between first and second measure in any of the evaluated parameters in both OCT's ($p > 0.05$). Table 2 shows the repeatability for thickness measurements in the macular region within each instrument.

Table 2. Repeatability of macular measurements.

	Canon OCT-HS100					Zeiss Cirrus HD-OCT 5000				
Thickness (µm)	**Mean**	**CR**	**CR%**	**R^2**	**p**	**Mean**	**CR**	**CR%**	**R^2**	**p**
Center	276.22 ± 15.69	5.04	1.82	0.97	0.95	259.34 ± 15.97	2.57	0.99	0.99	0.55
Inner superior	351.08 ± 12.07	2.82	0.80	0.98	0.99	324.82 ± 11.48	5.25	1.62	0.95	0.36
Inner nasal	352.02 ± 14.13	3.11	0.88	0.99	0.07	327.27 ± 13.72	4.28	1.31	0.97	0.36
Inner inferior	347.33 ± 10.99	4.46	1.28	0.95	0.71	322.38 ± 11.99	4.05	1.26	0.97	0.58
Inner temporal	335.34 ± 10.82	2.09	0.62	0.99	0.90	311.41 ± 10.57	4.20	1.35	0.96	0.15
Outer superior	305.21 ± 12.17	8.58	2.81	0.89	0.16	277.65 ± 12.42	6.65	1.67	0.96	0.38
Outer nasal	317.66 ± 14.57	2.98	0.94	0.99	0.29	295.48 ± 14.24	3.57	1.21	0.98	0.44
Outer inferior	290.74 ± 12.22	4.80	1.65	0.97	0.35	267.27 ± 14.21	3.73	1.40	0.98	0.26
Outer temporal	287.54 ± 10.17	4.00	1.39	0.96	0.69	258.96 ± 9.55	4.70	1.81	0.93	0.50

CR = coefficient of repeatability; CR% = coefficient of repeatability as a percentage of mean

5.1.2 Between instrument comparison

For the optic disc measurements, the R^2 values ranged between 0.66 and 0.97, however there was no statistical difference in CR values between Canon OCT-HS100 and Zeiss Cirrus HD-OCT ($p > 0.05$). For the OCT-derived thickness measures in the macula, R^2 ranged between 0.43 and 0.96 and there was a statistical difference in thickness values between the two instruments ($p < 0.05$). Canon measured thicker values for all macular parameters compared with Zeiss (Table 3).

Table 3. Comparison in repeatability between Canon OCT-HS100 and Zeiss Cirrus HD-OCT 5000. Positive values and negative values imply greater/thicker measurements and lower/thinner measurements with Canon respectively.

Optic disc	**Mean difference (p-value)**	**R^2 (p-value)**
Disc area (mm^2)	0.22 ($p > 0.05$)	0.80 ($p < 0.05$)
Rim area (mm^2)	0.17 ($p > 0.05$)	0.73 ($p < 0.05$)
Cup volume (mm^3)	-0.03 ($p > 0.05$)	0.97 ($p < 0.05$)
Cup/Disc vertical ratio	-0.03 ($p > 0.05$)	0.85 ($p < 0.05$)
RNFL average (µm)	5.20 ($p > 0.05$)	0.87 ($p < 0.05$)
RNFL Inferior (µm)	5.36 ($p > 0.05$)	0.82 ($p < 0.05$)
RNFL Superior (µm)	5.43 ($p > 0.05$)	0.67 ($p < 0.05$)
RNFL Nasal (µm)	8.02 ($p > 0.05$)	0.69 ($p < 0.05$)
RNFL Temporal (µm)	4.00 ($p > 0.05$)	0.66 ($p < 0.05$)
Macula		
Center (µm)	16.87 ($p < 0.05$)	0.96 ($p < 0.05$)
Inner superior (µm)	26.25 ($p < 0.05$)	0.43 ($p < 0.05$)
Inner nasal (µm)	24.74 ($p < 0.05$)	0.62 ($p < 0.05$)
Inner inferior (µm)	24.95 ($p < 0.05$)	0.53 ($p < 0.05$)
Inner temporal (µm)	23.93 ($p < 0.05$)	0.67 ($p < 0.05$)
Outer superior (µm)	27.55 ($p < 0.05$)	0.59 ($p < 0.05$)
Outer nasal (µm)	22.18 ($p < 0.05$)	0.60 ($p < 0.05$)
Outer inferior (µm)	23.46 ($p < 0.05$)	0.62 ($p < 0.05$)
Outer temporal (µm)	28.58 ($p < 0.05$)	0.64 ($p < 0.05$)

RNFL = retinal nerve fiber layer

5.2 PAPER II

5.2.1 Comparison of pRNFL parameters between MS subtypes and HCs

The average pRNFL thickness and pRNFL thickness in the four quadrants around the optic nerve head were compared between MS eyes and eyes of HCs. The group of HCs were set as reference in the analysis. The total MS cohort of 465 patients was divided into subtypes and consisted of 336 RRMS (72%), 112 (24%) SPMS and 17 (4%) PPMS patients. The demographics of study participants is presented in Table 4. A statistically significant thickness loss, compared with HCs, was seen in all MS subtypes and in all pRNFL parameters except in the superior quadrant of PPMS. The average pRNFL was 6.4 µm thinner (95% CI -8.5 to -4.3 µm, $p < 0.001$) in RRMS, 11.6 µm thinner (95% CI -14.4 to -8.8 µm, $p < 0.001$) in SPMS and 10.7 µm thinner (95% CI -16.0 to -5.5 µm, $p < 0.001$) in PPMS compared to HCs. A significantly thinner pRNFL thickness was seen in all quadrants in RRMS and SPMS. The largest thickness difference compared to HCs was found in the T-pRNFL of PPMS patients with a mean reduction of 15.8 µm (95% CI -21.4 to -10.1 µm).

Table 4. Demographics of study participants.

	HCs (n=168)	RRMS (n=336)	SPMS (n=112)	PPMS (n=17)
Age at OCT date (mean ± SD)	42.3 ± 15.4	38.9 ± 9.7	53.8 ± 10.0	50.2 ± 13.2
Sex (% female)	76.7	70.8	65.4	55.6
Disease duration (mean years ± SD)		9.1 ± 7.2	21.8 ± 9.4	10.6 ± 8.3
Disease modifying treatment duration 1st line (mean years ± SD)		2.8 ± 37	5.6 ± 6.3	2.5 ± 5.0
Disease modifying treatment duration 2nd line (mean years ± SD)		1.4 ± 2.1	1.3 ± 2.3	0.2 ± 0.4
EDSS median (interquartile range)		2.0 (1.5)	5.5 (2.8)	5.5 (2.0)
% of eyes with previous history of ON in one eye		87 (26.5%)	24 (18.9%)	0 (0%)
% of eyes with previous history of ON in both eyes		23 (6.2%)	8 (6.3%)	0 (0 %)

HCs = healthy controls, RRMS = relapsing remitting multiple sclerosis, SPMS = secondary progressive multiple sclerosis, PP = primary progressive multiple sclerosis, OCT = optical coherence tomography, EDSS = expanded disability status scale, ON = optic neuritis

5.2.2 Comparison of average pRNFL thickness in eyes with and without ON history and HCs

MS eyes with history of ON (MSON+) had the most reduced pRNFL thickness with an average of 80 µm. MS eyes without prior ON (MSON-) showed similar thickness values as the unaffected fellow eye of MSON+ (93 µm versus 94.5 µm). HCs had an average pRNFL thickness of 99 µm.

5.2.3 Association between pRNFL parameters and physical and cognitive dysfunction

A statistical association was found between EDSS and average pRNFL ($p < 0.01$) and T-pRNFL ($p < 0.01$) thicknesses. For every increase in EDSS score, i.e. increased neurological disability, the average pRNFL was reduced by 1.0 µm (95% CI -1.7 to -0.2) and the T-pRNFL thickness decreased by 1.2 µm (95% CI -2.0 to -0.5). A borderline association was found between EDSS and the inferior quadrant of pRNFL (-1.2 µm (95% CI -2.3 to 0.0; $p < 0.05$)). No statistical relationship was found between EDSS and pRNFL thickness in the superior and nasal quadrants. A statistically significant relationship was mainly found between SDMT score and the T-pRNFL quadrant. The T-pRNFL was reduced by 0.2 µm (95% CI 0.1 to 0.3; $p < 0.01$) with every point of decrease in SDMT score, i.e. worsening of cognition (Table 5). No statistical association could be found between MSIS-29 physical or psychological scores and any of the pRNFL parameters.

Table 5. Peripapillary retinal nerve fiber layer thickness difference between multiple sclerosis subtypes and healthy controls. The relationship between optical coherence tomography measures and clinical assessment scales are shown. The values in the boxes of the assessment scales include the entire multiple sclerosis cohort and reflect best-fit slopes with units of microns/scale points.

	Peripapillary retinal nerve fiber layer thickness difference (µm)				
	Average	Quadrants			
		Superior	Nasal	Inferior	Temporal
Disease subtype †					
HCs	Ref. 99 µm ± 9.7	Ref. 120 µm ± 13.8	Ref. 83 µm ± 14.7	Ref. 127 µm ± 16.6	Ref. 71 µm ± 11.1
RR	-6.4 (-8.5 to -4.3) ***	-5.5 (-8.3 to -2.7) ***	-5.9 (-10.5 to -3.9) ***	-7.2 (-10.5 to -3.9) ***	-7.6 (-9.8 to -5.3) ***
SP	-11.6 (-14.4 to -8.8) ***	-11.2 (-19.0 to -8.4) ***	-8.1 (-18.9 to -10.2) ***	-14.5 (-18.9 to -2.3) ***	-13.2 (-16.2 to -10.3) ***
PP	-10.7 (-16.0 to -5.5) ***	-4.7 (-11.9 to 2.4)	-10.7 (-18.9 to 2.3) ***	-10.6 (-18.9 to -2.3) *	-15.8 (-21.4 to -10.1) ***
EDSS ǂ	-1.0 (-1.7 to -0.2) **	-0.8 (-1.8 to 0.2)	-0.7 (-1.5 to 0.1)	-1.2 (-2.3 to 0.0) *	-1.2 (-2.0 to -0.5) **
SDMT ǂ	0.1 (0.0 to 0.2) *	0.1 (0.0 to 0.2)	0.0 (-0.1 to 0.1)	0.2 (0.0 to 0.3) *	0.2 (0.1 to 0.3) **
MSIS-29 ǂ					
Physical Scale	-0.30 (-1.71 to 1.10)	-0.5 (-2.33 to 1.36)	0.1 (-1.45 to 1.69)	-0.9 (-3.07 to 1.30)	0.1 (-1.35 to 1.47)
Psychological Scale	0.1 (-1.12 to 1.35)	-0.1 (-1.68 to 1.55)	-0.1 (-1.45 to 1.30)	0.3 (-1.65 to 2.19)	0.4 (-0.79 to 1.68)

HCs = healthy controls, RR = relapsing remitting, SP = secondary progressive, PP = primary progressive, EDSS = expanded disability status scale, SDMT = symbol digit modalities test, MSIS-29 = multiple sclerosis impact scale 29 † Adjusted for age, sex and previous history of optic neuritis. ǂ Only MS patients were included and a correction for MS subtype, disease duration, age, sex, duration of exposure to disease modifying treatments was done. * For $p < 0.05$, ** for $p < 0.01$, and *** for $p < 0.001$

5.3 PAPER III

5.3.1 Comparison of OCT parameters between MS patients and HCs

Demographics of the 546 MS patients and 175 HCs are presented in Table 6. Most MS patients had RRMS (72%), followed by SPMS (25%) and PPMS (3%). Seventy percent of the MS cohort and ~76% of the HCs were female. The progressive types of MS showed significantly higher EDSS scores and significantly lower SDMT scores compared with RRMS ($p < 0.001$ respectively). Approximately 19% of patients with RRMS had a history of previous ON in one eye and almost 7% had prior ON in both eyes. In the SPMS group approximately 15% had prior ON in one eye and 4% had ON in both eyes.

All analyzed OCT parameters (average pRNFL, T-pRNFL, inner GCC and inner GCIP thicknesses) were significantly reduced in thickness in all MS eyes as a group and in each subtype, compared with HCs. However, as shown in Table 7, T-pRNFL and inner GCC had strong p-values and the highest regression coefficients in differentiating MS subtypes from HCs. The highest regression coefficient was found for the T-pRNFL in PPMS patients with a reduction of 16.31 μm ($p < 0.001$) compared with HCs.

Table 6. Demographics of study participants.

	HCs (n=175)	**PP (n=19)**	**RR (n=391)**	**SP (n=136)**
Age (mean ± SD)	42.5 ± 15.4	51.8 ± 13.9	38.8 ± 9.5	54.7 ± 10.1
Sex (% female)	76.6	57.9	70.8	66.9
Disease duration (mean years ± SD)	---	11.2 ± 7.9	8.8 ± 7.1	22.9 ± 10
Treatment duration 1st line (mean years ± SD)	---	2.3 ± 4.7	2.7 ± 3.7	5.5 ± 6.1
Treatment duration 2nd line (mean years ± SD)	---	0.3 ± 0.6	1.3 ± 2.0	1.2 ± 2.3
EDSS at baseline, (median (IQR))	---	6 (2)	2 (1.5)	5.5 (2.5)
SDMT at baseline, (median (IQR))	---	50 (11)	57 (15)	47 (27)
MSIS-29 at baseline, (mean (± SD))	---			
Physical scale		2.8 ± 0.8	1.7 ± 0.8	2.7 ± 0.9
Psychological scale		2.4 ± 0.9	2.1 ± 0.9	2.5 ± 0.9
Previous history of ON in one eye, %	---	0	18.8	15.4
Previous history of ON in both eyes, %	---	0	6.6	4.4

PP: primary progressive, RR: relapsing remitting, SP: secondary progressive, HCs: healthy controls.

Table 7. Average reduction in thickness of optical coherence tomography measures in 19 primary progressive (PP), 391 relapsing remitting (RR) and 136 secondary progressive (SP) multiple sclerosis patients compared with 175 healthy controls (HCs).

	Average pRNFL (µm)		**T-pRNFL (µm)**		**Inner GCC (µm)**		**Inner GCIP (µm)**	
HCs	Ref.	*P*-value	Ref.	*P*-value	Ref.	*P*-value	Ref.	*P*-value
MS All subtypes	-7.58	< 0.001	-9.35	< 0.001	-8.24	< 0.001	-6.31	< 0.001
RR	-6.29	< 0.001	-7.74	< 0.001	-6.38	< 0.001	-4.97	< 0.001
SP	-11.29	< 0.001	-13.07	< 0.001	-12.79	< 0.001	-9.81	< 0.001
PP	-9.18	0.009	-16.31	< 0.001	-12.16	< 0.001	-7.86	< 0.001

pRNFL: peripapillary retinal nerve fiber layer; T-pRNFL: temporal peripapillary retinal nerve fiber layer; GCC: ganglion cell complex, GCIP: ganglion cell–inner plexiform layer. Coefficient from generalized estimation equation models adjusted for age, sex, and previous history of optic neuritis.

5.3.2 Association between OCT parameters and physical and cognitive dysfunction

Physical disability as measured with EDSS was associated with all four OCT measures after controlling for potential confounders including MS subtype, sex, age, disease duration, previous ON history, and duration of DMTs. The highest regression coefficient was seen in the inner GCC with a reduction of 1.78 µm ($p < 0.001$) for every increased EDSS score. Inner GCC was followed by T-pRNFL and inner GCIP with a reduction of 1.52 µm ($p < 0.001$) and 1.28 µm, ($p < 0.001$), respectively. Higher SDMT scores, i.e. better cognitive performance, were associated with greater thicknesses in all four OCT measures. The OCT measure showing highest association with SDMT was T-pRNFL thickness with a regression coefficient of 0.17 µm ($p < 0.001$). The analysis including only MS eyes without prior ON did not influence the results for neither EDSS or SDMT. No statistical association could be found between MSIS-29 physical or psychological scores and any of the OCT measures (Table 8).

Table 8. The association between baseline OCT-derived thickness measures of MS eyes, including the entire MS group, and different assessment scales.

All eyes (Models are adjusted for previous history of optic neuritis)	**Average pRNFL thickness (µm)**		**Temporal pRNFL thickness (µm)**		**Inner GCC thickness (µm)**		**Inner GCIP thickness (µm)**	
EDSS score	-1.08	*P* < 0.001	-1.27	*P* < 0.001	-1.77	*P* < 0.001	-1.32	*P* < 0.001
SDMT score	0.14	*P* = 0.001	0.16	*P* < 0.001	0.11	*P* = 0.02	0.07	*P* = 0.04
MSIS-29 Physical scale	-0.34	*P* = 0.64	0.15	*P* = 0.83	-1.03	*P* = 0.16	-0.88	*P* = 0.11
MSIS-29 Psychological scale	0.16	*P* = 0.81	0.55	*P* = 0.37	-0.59	*P* = 0.36	-0.66	*P* = 0.17
In eyes with no history of optic neuritis	**Average pRNFL thickness (µm)**		**Temporal pRNFL thickness (µm)**		**Inner GCC thickness (µm)**		**Inner GCIP thickness (µm)**	
EDSS score	-1.06	*P* = 0.006	-1.52	*P* < 0.001	-1.78	*P* < 0.001	-1.28	*P* < 0.001
SDMT score	0.14	*P* = 0.001	0.17	*P* < 0.001	0.12	*P* = 0.02	0.08	*P* = 0.05

EDSS: expanded disability status scale, SDMT: symbol digit modalities test, MSIS 29 = multiple sclerosis impact scale 29, pRNFL: peripapillary retinal nerve fiber layer; T-pRNFL: temporal peripapillary retinal nerve fiber layer; GCC: ganglion cell complex, GCIP: ganglion cell–inner plexiform layer.

5.3.3 Longitudinal analysis of OCT parameters and future disability worsening

The patients with reduced OCT thickness had an average of 0.7 EDSS (0.51-0.87) scores higher than the patients with normal OCT thickness over the 36-month follow-up time and the results were statistically significant. Also, the patients with reduced OCT thickness performed with an average of 4.4 (4.1-4.9) SDMT scores lower than the patients with normal OCT thickness during the follow-up time and the difference was statistically significant. Overall, it was not possible to predict future physical disability and/or cognitive impairment since patients with reduced or normal baseline OCT thickness were almost parallel over the follow-up time in both EDSS and SDMT (Figures 9 and 10).

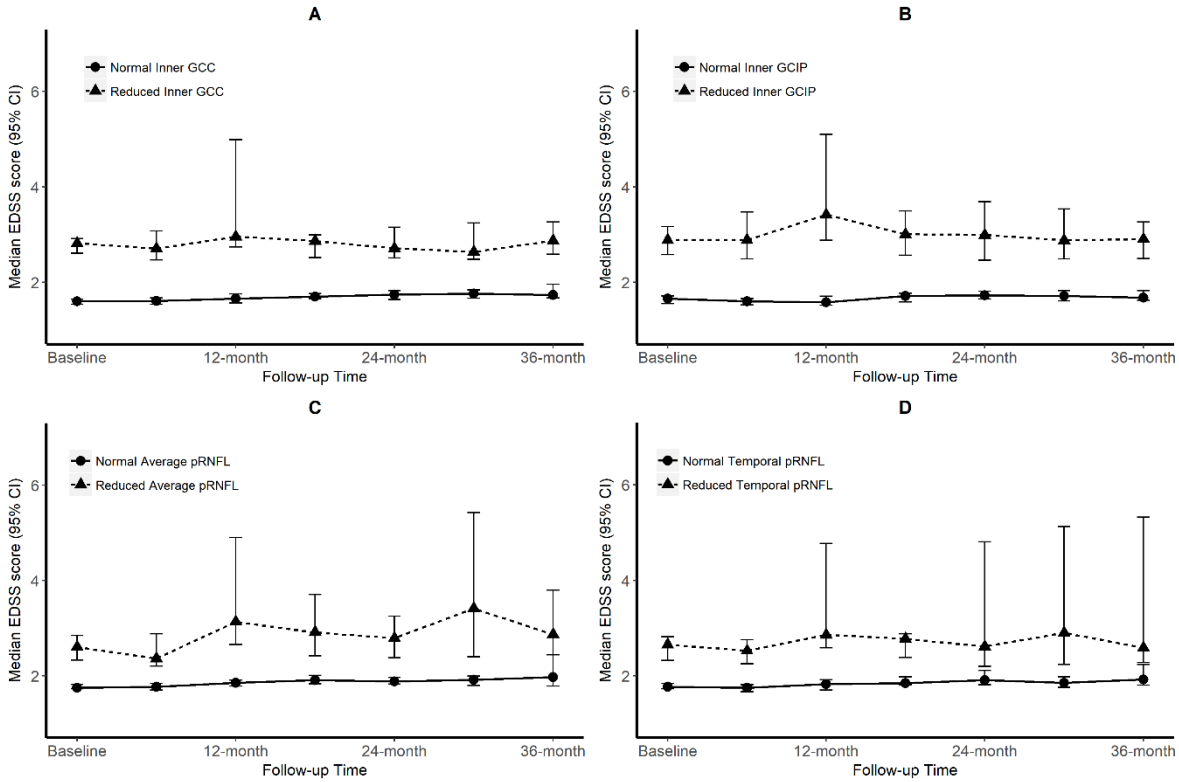

Figure 9. Progression of physical disability measured with expanded disability status scale (EDSS) according to baseline optical coherence tomography (OCT) measures over a 36-month period: **A.)** Inner ganglion cell complex (GCC), **B.)** Inner ganglion cell-inner plexiform layer (GCIP), **C.)** Average peripapillary retinal nerve fiber layer (pRNFL), **D.)** Temporal peripapillary retinal nerve fiber layer (Temporal pRNFL). "Normal" values for each OCT measure was defined as within one standard deviation of each measure in healthy control eyes and "reduced" was two or more standard deviations lower than healthy control eyes.

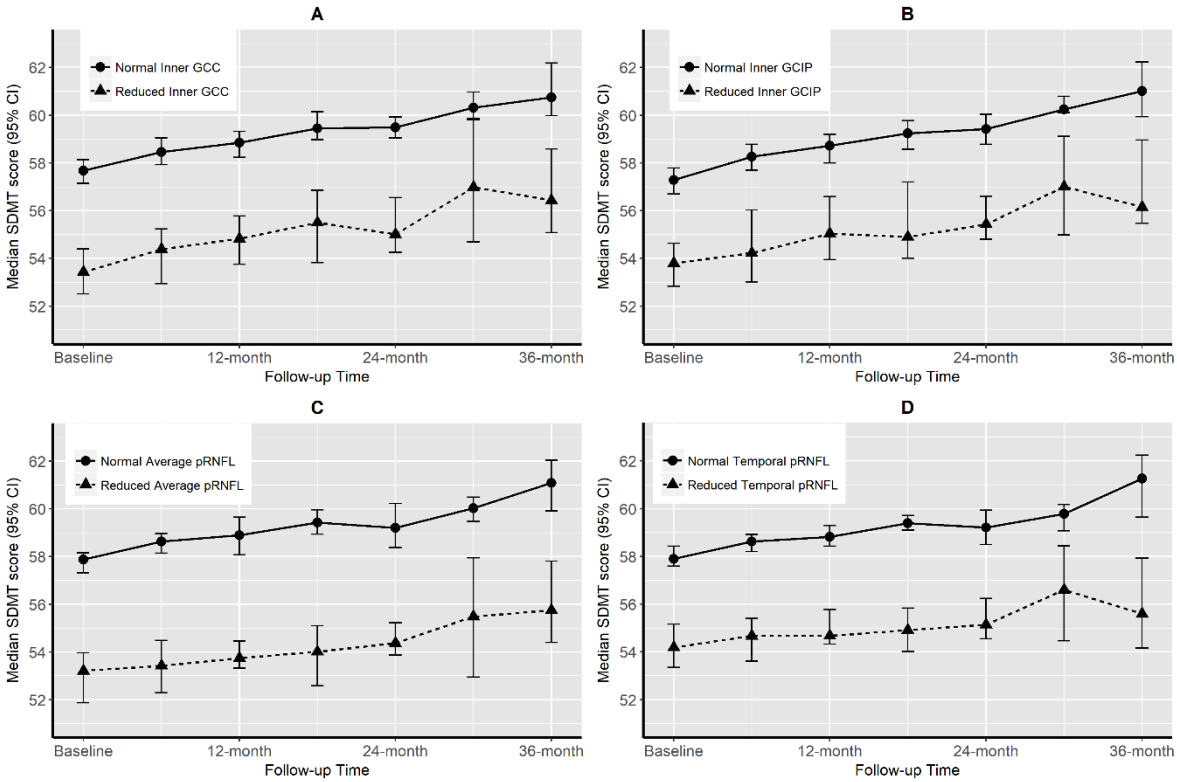

Figure 10. Progression of cognitive impairment measured with symbol digit modalities test (SDMT) according to the baseline optical coherence tomography (OCT) measures over a 36-month period: **A.)** Inner ganglion cell complex (GCC), **B.)** Inner ganglion cell-inner plexiform layer (GCIP), **C.)** Average peripapillary retinal nerve fiber layer (pRNFL), **D.)** Temporal peripapillary retinal nerve fiber layer (Temporal pRNFL). "Normal" values for each OCT measure was defined as within one standard deviation of each measure in healthy control eyes and "reduced" was two or more standard deviations lower than healthy control eyes.

6 DISCUSSION

The overall purpose of the three studies this thesis is based on was to investigate the potentials of OCT as a non-invasive tool for monitoring MS patients and measuring physical disability and cognitive impairment. Because of the recently developed segmentation algorithms, which are incorporated into the OCT, it is possible to automatically quantify the thickness of different retinal layers. Since the usefulness of an instrument depends strongly on its test-retest reliability it was important to firstly evaluate the new Canon-OCT HS100 with its automatic eye tracking function and compare it with the well-established Zeiss Cirrus HD-OCT 5000. The automatic eye track system remembers the previous scan area on the retina and will automatically position on the same location during follow-up examinations. To have each image at the exact location is a big advantage when monitoring progression of retinal pathologies and when comparing scans from previous examinations, such as monitoring retinal thickening over time. This automatic system makes the scan procedure quicker and easier for the operator since it immediately recovers its position on the retina if the patient blinks or changes fixation. In Paper I the optic disc and macular parameters were found to be repeatable in both instruments, however slightly better with the Zeiss Cirrus HD-OCT. The CR% range decreased in both OCTs when the cup volume parameter was excluded. The cup volume was also the least repeatable parameter in our previous study with the same OCTs (103). The CR% values of the macular parameters for both OCTs had a smaller range than the optic disc parameters, i.e. the variation was less, and the repeatability was better in the macular region than in the optic disc. This probably has an anatomical explanation. Unlike the macular region, the appearance of the optic disc often varies a lot among individuals. The presence of blood vessels may interfere the optic disc measurements. This makes it more difficult to identify the structures properly and the variation increases (104). In addition, tilted disc and peripapillary crescent, which are common features among myopes, might also influence the measurements since it might be difficult for the OCT to correctly define the optic disc margin. It is difficult to compare measurements obtained from different OCTs because of different wavelengths, scan speed and axial resolution. With higher resolution it is more difficult to replicate the segmentation. This might explain why the repeatability is slightly better with Zeiss, which has lower resolution than Canon.

Although the correlation between Canon-OCT HS100 and Zeiss Cirrus HD-OCT was good, the thickness estimation was different between the two instruments. This is in line with a previous study investigating macular thickness with six different OCTs, including Cirrus HD-OCT, in healthy subjects (105). Canon-OCT HS100 reported slightly thicker values than Zeiss Cirrus HD-OCT in almost all the evaluated parameters, especially in the macular region. Only the cup volume and cup/disc vertical ratio values were larger with the Zeiss Cirrus HD-OCT. This difference in quantitative estimation between different OCTs is important to have in mind when interpreting the results. It is therefore necessary to use the same device when monitoring a patient over time, i.e. OCTs are not interchangeable. Smaller disc scan diameter increases the risk of measuring close to the optic nerve head border which is an area with thicker pRNFL (106). This might explain why Canon, with slightly smaller

disc scan diameter than Zeiss (3.45 mm vs. 3.46 mm), gave rise to thicker pRNFL values. The macular thickness measurements were approximately 24 µm thicker when measured with Canon. This is most likely explained by the differences in the segmentation software for the instruments, i.e. different reference planes are used (105). Canon defines the retinal thickness from ILM to the outer border of RPE whereas Zeiss measures the thickness from ILM to the center of the RPE layer.

In paper II and III the purpose was to investigate the thickness of different OCT measures in all MS subtypes compared with HCs and to correlate these measures with functional tests. Paper II focused on the pRNFL thickness, which was the retinal structure that was initially investigated in MS-OCT studies. However, most studies have included small cohorts and/or not included all MS subtypes. In addition, many studies applied the older generation of OCT. Both paper II and III present large single-center cohorts with all MS subtypes included. To the best of our knowledge, only the study by Gelfand et al. have had a larger single-center MS cohort (52). Regarding pRNFL, in paper III we chose to focus on the overall average value and T-pRNFL and did not analyze the other quadrants. This was based on our results from paper II. Some patients find it very difficult to fixate on the target during the optic disc image acquisition and this can make it difficult to obtain high quality images. Therefore, it was interesting to investigate if the thickness reduction in the macular region of MS patients differed from the HCs as much as T-pRNFL. Due to the newly developed segmentation algorithms it was possible to automatically quantify the macular GCIP and macular GCC thicknesses. In paper III we also investigated the predictive value of baseline OCT measures over a 36-month period.

The effect of previous ON on pRNFL thickness was evaluated in paper II. MSON+ eyes had approximately 20 µm reduction of pRNFL thickness compared to HCs. This finding is in accordance with previous studies and was not surprising since it is well established that ON has a great impact on pRNFL (3, 79, 81). It has been discussed that the MSON+ eye might influence the pRNFL of the fellow eye. This is caused by the ON lesion in the MSON+ eye spreading into the chiasm leading to pRNFL thinning of the fellow eye (87). It is not well described in the literature how much the pRNFL in the fellow eye of MSON+ eye might be reduced. To investigate this, we separated the fellow eyes without ON history and compared the mean thickness values between the groups. The MSON+ fellow eye was shown to have a similar pRNFL thickness reduction as MSON- eyes. In other words, a reduction was seen in the fellow eyes of MSON+ eyes, however the thinning was not larger than in the MS patients without ON history in either eye. ON within 6 months prior to OCT assessment was an exclusion criterium in our analyzes. This is common feature in MS-OCT studies since the retinal atrophy following an ON attack is not stabilized until 6 months after onset (75, 107). The pRNFL is also known to swell during an on-going ON and the true reduction might be masked due to initial edema in the acute phase (first 3 months). The macular GCIP has been proposed to be superior to pRNFL for early detection of retinal atrophy in acute ON since it is not influenced by edema (78, 108, 109).

Except for the superior quadrant of PPMS, paper II showed a statistically significant thinning of pRNFL for all MS subtypes compared with HCs and this is in agreement with previous publications (52, 79, 110). Although all quadrants were reduced in thickness compared with HCs, they were not equally affected. The average pRNFL is calculated from the average values of each quadrant. This might weaken an existing association and average pRNFL is therefore not the most sensitive pRNFL parameter. The largest pRNFL thickness reduction compared with HCs was seen in the T-pRNFL of PPMS with an average decrease of 15.8 µm. In paper III we reported that both pRNFL and GCIP thickness were reduced in MS patients compared to HCs, which is in line with other studies (111-113) and that the T-pRNFL was the most reduced parameter in all MS subtypes. The largest reduction was found in PPMS patients with an average decrease of 16.3 µm compared with HCs. The inner GCIP was the parameter with the lowest regression coefficients, ranging from -4.97 µm to -9.81 µm. This might be due to the combined measurement with the inner plexiform layer masking the true reduction of ganglion cells. Previous publications have also reported the T-pRNFL to be more reduced than the other quadrants in MS patients (52, 80). The thickness reduction of T-pRNFL reported with OCT is supported by the post mortem findings by Evangelou et al. (114). They reported that the axons from parvocellular neurons, which are the predominant axons of the papillomacular bundle (temporal portion of the pRNFL), showed the largest reduction in MS eyes. It is unknown why a preferential damage of axons is found in the temporal quadrant. These axons of the parvocellular pathway might be more vulnerable to MS damage (52). Another theory is that MS lesions in the visual cortex might cause thinning of the T-pRNFL since the central visual field is highly subserved by the visual cortex. This increases the possibility that MS lesions in the posterior visual pathway will damage the axons supplying the central visual field, i.e. the T-pRNFL (87). PPMS patients do not suffer from relapses and therefore have no ON history. Based on our results, we conclude that another process, such as retrograde trans-synaptic degeneration or primary retinal pathology, might be responsible for the retinal atrophy seen in these patients.

Ten years ago, Toledo et al. investigated the relationship between pRNFL and physical disability and cognitive impairment in MS (115). Both average pRNFL and T-pRNFL were associated with EDSS. However, the study was performed by the time of the older generation of OCT. Paper II has also shown associations between pRNFL and clinical measures. Physical disability, measured with EDSS, was in paper II inversely correlated with average pRNFL, inferior pRNFL and T-pRNFL. The highest regression coefficients and p-values were found between T-pRNFL, inferior pRNFL and EDSS. Since the T-pRNFL suffers a larger proportional loss of axons than the inferior quadrant, changes in T-pRNFL might be easier to detect in a clinical setting. Regarding the EDSS scores in paper III, the inner GCC and T-pRNFL had the highest regression coefficients and equally strong p-values. Other SD-OCT studies in the MS field have also reported associations between different OCT measures and EDSS. Albrecht et al. found that average pRNFL and total macular thickness correlated with EDSS (84). Garcia-Martin et al. reported inverse correlations between thinning of pRNFL and GCIP thicknesses and EDSS scores. Also, the GCIP thickness could predict

axonal loss in MS patients (116). Same author reported a correlation between pRNFL thinning in the superior quadrant and T-pRNFL and EDSS increase over 5 years in RRMS patients (117). Another study that only included RRMS patients with EDSS ≤ 3; ≥ 15 years could not find a correlation between pRNFL thickness and EDSS. However, this might be due to the limited range of EDSS scores (118). The inner GCC is a macular measurement and based on our results, it might be an alternative to use this parameter instead of T-pRNFL in those patients who have difficulties to fixate during optic disc measurements.

The relationship between cognitive impairment and OCT parameters have so far only been sparsely investigated. Cognitive impairment, measured with SDMT, was mostly associated with the inferior quadrant and T-pRNFL in paper II and with T-pRNFL in paper III. Toledo et al. evaluated different TD-OCT measures and they observed that the average pRNFL, and especially the T-pRNFL, were correlated with several cognitive measures. The strongest correlation was found between T-pRNFL and SDMT (115). A cross-sectional study by Coric et al., analyzed average pRNFL and macular GCIP in MS patients. They reported a significant association between these OCT measures and cognitive impairment (119).

Garcia-Martin et al. reported that T-pRNFL thinning was associated with reduced quality of life. In both paper II and paper III no correlation was found between MSIS-29 and any of the investigated OCT parameters (117). Important differences compared to our study was that they only included patients with RRMS and used another patient reported outcome.

The purpose with the longitudinal analysis in paper III was to investigate if the baseline OCT measure could predict future worsening in physical disability and/or cognitive impairment in MS. However, we did not observe any obvious differences in the rate of change for patients with reduced or normal baseline OCT measures. The results might have been different with a shorter disease duration since the GCIP thinning has been shown to be more rapid in MS patients with a disease duration of less than 5 years (89). SDMT increased significantly by 1.2 scores on 6-month average over the follow-up time. This is explained by the learning effect which is a limitation with SDMT. The idea of using OCT as a predictor of future disability in MS has been evaluated in a few studies. Martinez-Lapiscina et al. demonstrated that patients with a pRNFL thickness equal to or below 87-88 µm had double the risk of disability worsening, measured with EDSS at any point after 1-3 years (33). Coric et al. reported increased odds of cognitive impairment in patients without ON history and reduced average pRNFL and GCIP thickness (119).

One strength with paper I was that we analyzed both macular and optic disc parameters in both instruments whereas many other studies have only focused on pRNFL or macular thickness. One limitation with paper I was that we did not investigate the inter-observer variability of Canon-OCT HS100. Strengths with paper II and paper III are the large sample size from one single neurology clinic, all MS subtypes were included, and we found OCT parameters that correlate with both physical disability and cognitive impairment in MS. One limitation with paper II is the cross-sectional design. In paper III we did not have the same number of patients through the whole 36-month period and this might influence the results.

Limitations in both paper II and paper III is the lack of CIS patients, the small number of PPMS patients and that the assessment of previous ON was only based on clinically confirmed episodes and patient self-reports.

6.1 CLINICAL RELEVANCE

Based on our results and similar previous studies, OCT might be a valuable and complementary imaging tool for MS patients. It is a reliable, fast and non-invasive technique, providing objective data on axonal and neuronal loss, showing that the retina is a mirror of the brain. With the automatic segmentation algorithms, the OCT operator is given a lot of information about the different retinal layers. More studies are needed over time to know which parameters are the most relevant for clinical practice and trials. However, based on our findings in combination with other published data, pRNFL and macular measurements, such as inner GCC, would be satisfying when studying neurodegeneration in MS patients. The T-pRNFL might be the best pRNFL parameter of choice when studying axonal loss related to MS. Since many studies, including Paper II and III, have demonstrated the T-pRNFL to be remarkably reduced compared to HCs. This is an important finding when differentiating between MS and other neurological diseases. Before the time of segmentation algorithms, total macular volume was the OCT parameter used for analysis of ganglion cells. Inner GCC and inner GCIP are more specific measurements than macular volume and therefore better to use when quantifying neuronal loss in MS.

Although the largest reduction of T-pRNFL was found in PPMS eyes, this group was the most difficult to include in our studies. Many of the PPMS patients coming to the clinic experienced great difficulties with muscle weakness and/or paralysis. This made it very difficult for them to participate in the OCT exam and therefore they could not be included. As already mentioned, OCT has many practical advantages, however it should be noted that it has limitations when examining MS patients with high EDSS scores.

6.2 FUTURE PERSPECTIVES

This thesis focused on investigating the role of OCT as a structural measurement in MS patients. Brain volume loss, measured with MRI, is a common measure when studying neurodegeneration in MS. Recent studies have suggested OCT as a complement to MRI when assessing neurodegeneration. The anterior visual pathway is an easy accessible part of the CNS to study the pathophysiology of MS. The ganglion cell layer is the neuronal part, i.e. brain gray matter and the RNFL consists of ganglion cell axons, i.e. brain white matter. To increase our knowledge about the potentials of OCT in MS it would not only be valuable to correlate it with MRI estimates and functional tests, but also to add OCT as an outcome measure for measuring treatment response in MS. Regarding functional tests, we only included EDSS and SDMT, which are normally a part of the routine examination of MS patients. Visual function tests, such as low contrast visual acuity, visual field and/or color vision should be added in future studies.

This thesis contributes with information about the use of OCT in MS and suggests OCT parameters to be associated with both physical disability and cognitive impairment. This thesis also confirms earlier cross-sectional studies that pRNFL thickness is significantly reduced in MS. The exploratory analysis of longitudinal data over a 36-month period could not predict future disability. Such longitudinal studies should focus on CIS or MS with a short disease duration. Following these patients over time is necessary to confirm if OCT might predict future disability worsening. RNFL and GCIP thickness have been the main focus in most published studies. Thickness measurements of deeper retinal layers have been performed sparsely in MS patients compared to HCs. The results have varied and therefore further studies are needed. A large post mortem study by Green et al. gives evidence for atrophy of the INL (82). The INL thickness and the use of OCT angiography will be of particular interest in MS studies focusing on inflammation.

7 CONCLUSIONS

- Canon OCT-HS100 reported thicker values for almost all investigated parameters compared with Zeiss Cirrus HD-OCT 5000. The difference was significant in the macular region with an average of 24 µm thicker values with Canon OCT-HS100. It is most likely due to different reference planes and this finding makes it clear that OCTs are not interchangeable.

- The pRNFL thickness in the unaffected fellow eye of MSON+ showed a similar reduction (-4.5 µm thinner than HCs) as the MS eyes without previous ON in any eye (-6 µm thinner than HCs).

- Axonal loss, measured as pRNFL thickness with OCT, could be demonstrated in all MS subtypes compared with HCs. The T-pRNFL of PPMS patients was the most reduced pRNFL quadrant compared with HCs with a mean reduction of 15.8 µm, ranging from -21.4 µm to -10.1 µm. Our results suggest that the T-pRNFL thickness might be an important measurement to differentiate MS subtypes.

- Retinal thickness reduction, measured with OCT, is associated with physical disability, assessed with EDSS, and with cognitive impairment, assessed with SDMT. T-pRNFL is the quadrant with the strongest association with both EDSS and SDMT according to the regression coefficients and p-values. Inner GCC was the macular OCT parameter with the highest association to these functional tests and might be a good option in patients with difficulties to participate in optic disc measurements.

8 ACKNOWLEDGMENTS

The process of earning a doctorate is long and demanding and is depending on the support from many individuals. I would like to reflect on those who have supported and helped me throughout the years as a PhD student.

Firstly, I would like to express my deep gratitude to my main supervisor, Associate Professor **Rune Brautaset** for your patient guidance, encouragement and immense knowledge. Thank you for believing in me and for making me a better researcher.

I am deeply grateful for all the help and support from my co-supervisors: Senior Lecturer Ph.D. **Maria Nilsson**, for the extensive knowledge about OCT and for all the countless spontaneous discussions about research over the years. M.D. Ph.D. **Max Albert Hietala**, for helping me to better understand multiple sclerosis and to see the whole picture outside the eye. Ph.D. **Marika Wahlberg Ramsay**, for your enthusiastic encouragement and motivation. Ph.D. **Ali Manouchehrinia**, for your patience and for the enormous help with the statistical analyzes.

I would like to express my appreciation to my co-authors: Professor **Fredrik Piehl** for sharing your great knowledge within the field of multiple sclerosis. I am very grateful to all my co-authors for the fruitful cooperation: **Petra Frehr Alstig**, **Petra Wikén**, Professor **Jan Hillert**, Professor **Tomas Olsson**, Professor **Ingrid Skelton Kockum**, Professor **Lou Brundin** and **Ori Zahavi**. It was a true pleasure working with all of you.

I would like to thank Ph.D. **Dheeraj Bansal** and **InnZ Medical** for the financial support during my doctoral education.

Professor **Jan Ygge** for valuable advice and for sharing your great knowledge.

Associate Professor **Tony Pansell** for motivation and always being friendly and helpful.

Ph.D. **Saber Abdi** for encouraging me when I was an Optometry student to aim for a Ph.D. I am truly grateful that you believed in me from the very first beginning.

I would like to thank my amazing colleagues, **Rebecka Rosén**, for all the support and for sharing this journey with me, Ph.D. **Alberto Domínguez Vicent**, for your endless help, **Kerstin Lutteman** for your encouragement and our many discussions and **Lovisa Pettersson**, for always being there spreading your positive energy and for contributing with illustrations in this thesis. I wish to thank all other wonderful colleagues at the Unit of Optometry: **Jaana Johansson**, **Annika Botes**, Ph.D. **Abinaya Venkataraman**, Ph.D. **Susanne Glimne**, Ph.D. **Anna Lindskoog Pettersson**, **Elin Bergling**, **Marie Brenning** and **Marguerite Tjärnberg**. It is a pleasure working with you all.

I am grateful to have had the opportunity to work with Ph.D. **Fredrik Källmark**, **Sten Lutteman, Ulla Bremö, Inga-Lill Thunholm-Henriksson** and **Monica Ferrato Sandén**.

I would like to thank the university administrators **Mia Pettersson** and **Susanne Jonson** for your help with practical matters.

I wish to thank my colleagues over the years at the emergency room at St. Erik Eye Hospital and the staff at Neuro Centrum at Karolinska Hospital in Solna.

I am very grateful to all study participants at St. Erik Eye Hospital and Neuro Centrum at Karolinska Hospital. Thank you for making this possible.

I am thankful for my lovely friends, **Elin, Linda, Marie** and **Therese**. You have always been there for me and I am grateful to have you in my life.

I would like to thank my parents, **Leif** and **Matilde**, and my sister, **Beatrice**, for always being there for me. Especially thanks to you, dad, for introducing me to science and for being my mentor.

Last but not least, I would like to thank the most important people in my life: My husband **Martin** and our children **Rafael** and **Vera**. Thank you for the endless love, support and patience throughout the years with all my talk about research, even during holidays. I could not have made it without you.

9 REFERENCES

1. Costello F, Van Stavern GP. Should optical coherence tomography be used to manage patients with multiple sclerosis? Journal of neuro-ophthalmology. 2012;32(4):363-71.
2. Frisen L, Hoyt WF. Insidious atrophy of retinal nerve fibers in multiple sclerosis. Funduscopic identification in patients with and without visual complaints. Archives of ophthalmology. 1974;92(2):91-7.
3. Petzold A, de Boer JF, Schippling S, Vermersch P, Kardon R, Green A, et al. Optical coherence tomography in multiple sclerosis: a systematic review and meta-analysis. The Lancet neurology. 2010;9(9):921-32.
4. Kolb H. The Organization of the Retina and Visual System. Chapter 1, Simple Anatomy of the Retina. Salt Lake City, Utah: University of Utah Health Sciences Center; 2005. p. 1, 2.
5. Nolte J. The human brain An introduction to its functional anatomy. Chapter 17, The visual system. St. Louis, Missouri: Mosby, Inc.; 2002. p. 417, 31-34.
6. Baylor DA. Photoreceptor signals and vision. Proctor lecture. Investigative ophthalmology & visual science. 1987;28(1):34-49.
7. Yau KW. Phototransduction mechanism in retinal rods and cones. The Friedenwald Lecture. Investigative ophthalmology & visual science. 1994;35(1):9-32.
8. Purves D, Augustine GJ, Fitzpatrick D, Hall WC, LaMantia A-S, McNamara JO, et al. Neuroscience. Chapter 11, Central visual pathways. Sunderland, Massachusetts: Sinauer Associates, Inc; 2004. p. 259-60, 70, 75.
9. Euler T, Haverkamp S, Schubert T, Baden T. Retinal bipolar cells: elementary building blocks of vision. Nature reviews Neuroscience. 2014;15(8):507-19.
10. Poche RA, Reese BE. Retinal horizontal cells: challenging paradigms of neural development and cancer biology. Development. 2009;136(13):2141-51.
11. Polyak S, Willmer EN. Retinal structure and colour vision. Documenta ophthalmologica Advances in ophthalmology. 1949;3:24-56.
12. Balasubramanian R, Gan L. Development of Retinal Amacrine Cells and Their Dendritic Stratification. Current ophthalmology reports. 2014;2(3):100-6.
13. Hansen JT. Netter's anatomy coloring book. Chapter 4, Visual system II. Philadelphia, Pennsylvania: Saunders Elsevier; 2010. p. 24.
14. Prasad S, Galetta SL. Anatomy and physiology of the afferent visual system. Handbook of clinical neurology. 2011;102:3-19.
15. Goga C, Ture U. The anatomy of Meyer's loop revisited: changing the anatomical paradigm of the temporal loop based on evidence from fiber microdissection. Journal of neurosurgery. 2015;122(6):1253-62.
16. Peltier J, Travers N, Destrieux C, Velut S. Optic radiations: a microsurgical anatomical study. Journal of neurosurgery. 2006;105(2):294-300.
17. Kamali A, Hasan KM, Adapa P, Razmandi A, Keser Z, Lincoln J, et al. Distinguishing and quantification of the human visual pathways using high-spatial-resolution diffusion tensor tractography. Magnetic resonance imaging. 2014;32(7):796-803.
18. Huang D, Swanson EA, Lin CP, Schuman JS, Stinson WG, Chang W, et al. Optical coherence tomography. Science. 1991;254(5035):1178-81.
19. Fercher AF, Hitzenberger CK, Drexler W, Kamp G, Sattmann H. In vivo optical coherence tomography. American journal of ophthalmology. 1993;116(1):113-4.
20. Swanson EA, Izatt JA, Hee MR, Huang D, Lin CP, Schuman JS, et al. In vivo retinal imaging by optical coherence tomography. Optics letters. 1993;18(21):1864-6.
21. Puliafito CA, Hee MR, Lin CP, Reichel E, Schuman JS, Duker JS, et al. Imaging of macular diseases with optical coherence tomography. Ophthalmology. 1995;102(2):217-29.

22. Adhi M, Duker JS. Optical coherence tomography-current and future applications. Current opinion in ophthalmology. 2013;24(3):213-21.
23. Jaffe GJ, Caprioli J. Optical coherence tomography to detect and manage retinal disease and glaucoma. American journal of ophthalmology. 2004;137(1):156-69.
24. Haouchine B, Massin P, Tadayoni R, Erginay A, Gaudric A. Diagnosis of macular pseudoholes and lamellar macular holes by optical coherence tomography. American journal of ophthalmology. 2004;138(5):732-9.
25. Voo I, Mavrofrides EC, Puliafito CA. Clinical applications of optical coherence tomography for the diagnosis and management of macular diseases. Ophthalmology clinics of North America. 2004;17(1):21-31.
26. Brown DM, Regillo CD. Anti-VEGF agents in the treatment of neovascular age-related macular degeneration: applying clinical trial results to the treatment of everyday patients. American journal of ophthalmology. 2007;144(4):627-37.
27. Bussel, II, Wollstein G, Schuman JS. OCT for glaucoma diagnosis, screening and detection of glaucoma progression. The British journal of ophthalmology. 2014;98:15-9.
28. Yaqoob Z, Wu J, Yang C. Spectral domain optical coherence tomography: a better OCT imaging strategy. BioTechniques. 2005;39:6-13.
29. Fujimoto J, Swanson E. The Development, Commercialization, and Impact of Optical Coherence Tomography. Investigative ophthalmology & visual science. 2016;57(9):1-13.
30. Lavinsky F, Lavinsky D. Novel perspectives on swept-source optical coherence tomography. International journal of retina and vitreous. 2016;2:25.
31. Kishi S. Impact of swept source optical coherence tomography on ophthalmology. Taiwan journal of ophthalmology. 2016;6(2):58-68.
32. Gao SS, Jia Y, Zhang M, Su JP, Liu G, Hwang TS, et al. Optical Coherence Tomography Angiography. Investigative ophthalmology & visual science. 2016;57(9):27-36.
33. Martinez-Lapiscina EH, Arnow S, Wilson JA, Saidha S, Preiningerova JL, Oberwahrenbrock T, et al. Retinal thickness measured with optical coherence tomography and risk of disability worsening in multiple sclerosis: a cohort study. The Lancet neurology. 2016;15(6):574-84.
34. Otani T, Yamaguchi Y, Kishi S. Improved visualization of Henle fiber layer by changing the measurement beam angle on optical coherence tomography. Retina. 2011;31(3):497-501.
35. Spaide RF, Curcio CA. Anatomical correlates to the bands seen in the outer retina by optical coherence tomography: literature review and model. Retina. 2011;31(8):1609-19.
36. Frohman EM, Fujimoto JG, Frohman TC, Calabresi PA, Cutter G, Balcer LJ. Optical coherence tomography: a window into the mechanisms of multiple sclerosis. Nature clinical practice Neurology. 2008;4(12):664-75.
37. Nakahara J, Maeda M, Aiso S, Suzuki N. Current concepts in multiple sclerosis: autoimmunity versus oligodendrogliopathy. Clinical reviews in allergy & immunology. 2012;42(1):26-34.
38. Compston A, Coles A. Multiple sclerosis. The Lancet. 2002;359(9313):1221-31.
39. Noseworthy JH, Lucchinetti C, Rodriguez M, Weinshenker BG. Multiple sclerosis. The New England journal of medicine. 2000;343(13):938-52.
40. Koch-Henriksen N, Sorensen PS. The changing demographic pattern of multiple sclerosis epidemiology. The Lancet neurology. 2010;9(5):520-32.
41. Kamm CP, Uitdehaag BM, Polman CH. Multiple sclerosis: current knowledge and future outlook. European neurology. 2014;72(3-4):132-41.

42. Ahlgren C, Oden A, Lycke J. High nationwide prevalence of multiple sclerosis in Sweden. Multiple sclerosis. 2011;17(8):901-8.
43. Ascherio A, Munger KL. Environmental risk factors for multiple sclerosis. Part I: the role of infection. Annals of neurology. 2007;61(4):288-99.
44. Hedstrom AK, Katsoulis M, Hossjer O, Bomfim IL, Oturai A, Sondergaard HB, et al. The interaction between smoking and HLA genes in multiple sclerosis: replication and refinement. European journal of epidemiology. 2017;32(10):909-19.
45. Ascherio A. Environmental factors in multiple sclerosis. Expert review of neurotherapeutics. 2013;13:3-9.
46. Brynedal B, Duvefelt K, Jonasdottir G, Roos IM, Akesson E, Palmgren J, et al. HLA-A confers an HLA-DRB1 independent influence on the risk of multiple sclerosis. PLoS One. 2007;2(7):e664.
47. Gough SC, Simmonds MJ. The HLA Region and Autoimmune Disease: Associations and Mechanisms of Action. Current genomics. 2007;8(7):453-65.
48. McFarland HF, Martin R. Multiple sclerosis: a complicated picture of autoimmunity. Nature immunology. 2007;8(9):913-9.
49. Cramer SP, Simonsen H, Frederiksen JL, Rostrup E, Larsson HB. Abnormal blood-brain barrier permeability in normal appearing white matter in multiple sclerosis investigated by MRI. Neuroimage clinical. 2014;4:182-9.
50. Sanchez I, Hassinger L, Paskevich PA, Shine HD, Nixon RA. Oligodendroglia regulate the regional expansion of axon caliber and local accumulation of neurofilaments during development independently of myelin formation. The journal of neuroscience. 1996;16(16):5095-105.
51. Tallantyre EC, Bo L, Al-Rawashdeh O, Owens T, Polman CH, Lowe JS, et al. Clinico-pathological evidence that axonal loss underlies disability in progressive multiple sclerosis. Multiple sclerosis. 2010;16(4):406-11.
52. Gelfand JM, Goodin DS, Boscardin WJ, Nolan R, Cuneo A, Green AJ. Retinal axonal loss begins early in the course of multiple sclerosis and is similar between progressive phenotypes. PLoS One. 2012;7(5):e36847.
53. Compston A, Coles A. Multiple sclerosis. The Lancet. 2008;372(9648):1502-17.
54. Patti F, Nicoletti A, Messina S, Bruno E, Fermo SL, Quattrocchi G, et al. Prevalence and incidence of cognitive impairment in multiple sclerosis: a population-based survey in Catania, Sicily. Journal of neurology. 2015;262(4):923-30.
55. Atlas SW, Grossman RI, Savino PJ, Schatz NJ, Sergott RC, Bosley TM, et al. Internuclear ophthalmoplegia: MR-anatomic correlation. American journal of neuroradiology. 1987;8(2):243-7.
56. Humm AM, Beer S, Kool J, Magistris MR, Kesselring J, Rosler KM. Quantification of Uhthoff's phenomenon in multiple sclerosis: a magnetic stimulation study. Clinical neurophysiology. 2004;115(11):2493-501.
57. Jasse L, Vukusic S, Durand-Dubief F, Vartin C, Piras C, Bernard M, et al. Persistent visual impairment in multiple sclerosis: prevalence, mechanisms and resulting disability. Multiple sclerosis. 2013;19(12):1618-26.
58. Cohen BA. Identification, causation, alleviation, and prevention of complications (ICAP): an approach to symptom and disability management in multiple sclerosis. Neurology. 2008;71:14-20.
59. Polman CH, Reingold SC, Banwell B, Clanet M, Cohen JA, Filippi M, et al. Diagnostic criteria for multiple sclerosis: 2010 revisions to the McDonald criteria. Annals of neurology. 2011;69(2):292-302.

60. Summers M, Fisniku L, Anderson V, Miller D, Cipolotti L, Ron M. Cognitive impairment in relapsing-remitting multiple sclerosis can be predicted by imaging performed several years earlier. Multiple sclerosis. 2008;14(2):197-204.
61. Miller DH, Chard DT, Ciccarelli O. Clinically isolated syndromes. The Lancet neurology. 2012;11(2):157-69.
62. Confavreux C, Vukusic S. Natural history of multiple sclerosis: a unifying concept. Brain. 2006;129:606-16.
63. Milo R, Kahana E. Multiple sclerosis: geoepidemiology, genetics and the environment. Autoimmunity reviews. 2010;9:387-94.
64. Tornes L, Conway B, Sheremata W. Multiple sclerosis and the cerebellum. Neurologic clinics. 2014;32(4):957-77.
65. Miller DH, Leary SM. Primary-progressive multiple sclerosis. The Lancet neurology. 2007;6(10):903-12.
66. Hillert J, Lycke J. Neurologi. Chapter 18, Multipel skleros. Stockholm: Liber AB; 2012. p. 385-7.
67. Toosy AT, Mason DF, Miller DH. Optic neuritis. The Lancet neurology. 2014;13(1):83-99.
68. Optic Neuritis Study Group. Multiple sclerosis risk after optic neuritis: final optic neuritis treatment trial follow-up. Archives of neurology. 2008;65(6):727-32.
69. Zimmermann H, Oberwahrenbrock T, Brandt AU, Paul F, Dörr J. Optical coherence tomography for retinal imaging in multiple sclerosis. Degenerative neurological and neuromuscular disease. 2014;4:153-62.
70. Kale N. Optic neuritis as an early sign of multiple sclerosis. Eye and brain. 2016;8:195-202.
71. Soderstrom M. Optic neuritis and multiple sclerosis. Acta ophthalmologica Scandinavica. 2001;79(3):223-7.
72. McDonald WI, Barnes D. The ocular manifestations of multiple sclerosis. 1. Abnormalities of the afferent visual system. Journal of neurology, neurosurgery, and psychiatry. 1992;55(9):747-52.
73. Beck RW, Cleary PA, Backlund JC. The course of visual recovery after optic neuritis. Experience of the Optic Neuritis Treatment Trial. Ophthalmology. 1994;101(11):1771-8.
74. Beck RW, Cleary PA. Optic neuritis treatment trial. One-year follow-up results. Archives of ophthalmology. 1993;111(6):773-5.
75. Costello F, Coupland S, Hodge W, Lorello GR, Koroluk J, Pan YI, et al. Quantifying axonal loss after optic neuritis with optical coherence tomography. Annals of neurology. 2006;59(6):963-9.
76. Fisher JB, Jacobs DA, Markowitz CE, Galetta SL, Volpe NJ, Nano-Schiavi ML, et al. Relation of visual function to retinal nerve fiber layer thickness in multiple sclerosis. Ophthalmology. 2006;113(2):324-32.
77. Trobe JD, Beck RW, Moke PS, Cleary PA. Contrast sensitivity and other vision tests in the optic neuritis treatment trial. American journal of ophthalmology. 1996;121(5):547-53.
78. Gabilondo I, Martinez-Lapiscina EH, Fraga-Pumar E, Ortiz-Perez S, Torres-Torres R, Andorra M, et al. Dynamics of retinal injury after acute optic neuritis. Annals of neurology. 2015;77(3):517-28.
79. Pulicken M, Gordon-Lipkin E, Balcer LJ, Frohman E, Cutter G, Calabresi PA. Optical coherence tomography and disease subtype in multiple sclerosis. Neurology. 2007;69(22):2085-92.

80. Sepulcre J, Murie-Fernandez M, Salinas-Alaman A, Garcia-Layana A, Bejarano B, Villoslada P. Diagnostic accuracy of retinal abnormalities in predicting disease activity in MS. Neurology. 2007;68(18):1488-94.
81. Petzold A, Balcer LJ, Calabresi PA, Costello F, Frohman TC, Frohman EM, et al. Retinal layer segmentation in multiple sclerosis: a systematic review and meta-analysis. The Lancet neurology. 2017;16(10):797-812.
82. Green AJ, McQuaid S, Hauser SL, Allen IV, Lyness R. Ocular pathology in multiple sclerosis: retinal atrophy and inflammation irrespective of disease duration. Brain. 2010;133:1591-601.
83. Gelfand JM, Nolan R, Schwartz DM, Graves J, Green AJ. Microcystic macular oedema in multiple sclerosis is associated with disease severity. Brain. 2012;135:1786-93.
84. Albrecht P, Ringelstein M, Muller AK, Keser N, Dietlein T, Lappas A, et al. Degeneration of retinal layers in multiple sclerosis subtypes quantified by optical coherence tomography. Multiple sclerosis. 2012;18(10):1422-9.
85. Klistorner A, Graham EC, Yiannikas C, Barnett M, Parratt J, Garrick R, et al. Progression of retinal ganglion cell loss in multiple sclerosis is associated with new lesions in the optic radiations. European journal of neurology. 2017;24(11):1392-8.
86. Balk LJ, Steenwijk MD, Tewarie P, Daams M, Killestein J, Wattjes MP, et al. Bidirectional trans-synaptic axonal degeneration in the visual pathway in multiple sclerosis. Journal of neurology, neurosurgery, and psychiatry. 2015;86(4):419-24.
87. Klistorner A, Sriram P, Vootakuru N, Wang C, Barnett MH, Garrick R, et al. Axonal loss of retinal neurons in multiple sclerosis associated with optic radiation lesions. Neurology. 2014;82(24):2165-72.
88. Saidha S, Al-Louzi O, Ratchford JN, Bhargava P, Oh J, Newsome SD, et al. Optical coherence tomography reflects brain atrophy in multiple sclerosis: A four-year study. Annals of neurology. 2015;78(5):801-13.
89. Ratchford JN, Saidha S, Sotirchos ES, Oh JA, Seigo MA, Eckstein C, et al. Active MS is associated with accelerated retinal ganglion cell/inner plexiform layer thinning. Neurology. 2013;80(1):47-54.
90. Zimmermann H, Freing A, Kaufhold F, Gaede G, Bohn E, Bock M, et al. Optic neuritis interferes with optical coherence tomography and magnetic resonance imaging correlations. Multiple sclerosis. 2013;19(4):443-50.
91. Grazioli E, Zivadinov R, Weinstock-Guttman B, Lincoff N, Baier M, Wong JR, et al. Retinal nerve fiber layer thickness is associated with brain MRI outcomes in multiple sclerosis. Journal of the neurological sciences. 2008;268(1-2):12-7.
92. Gordon-Lipkin E, Chodkowski B, Reich DS, Smith SA, Pulicken M, Balcer LJ, et al. Retinal nerve fiber layer is associated with brain atrophy in multiple sclerosis. Neurology. 2007;69(16):1603-9.
93. Kurtzke JF. Rating neurologic impairment in multiple sclerosis: An expanded disability status scale (EDSS). Neurology. 1983;33(11):1444.
94. Smith A. The Symbol Digit Modalities Test (SDMT) Symbol Digit Modalities Test: manual. Los Angeles: Western Psychological Services. 1982:1-3.
95. Charvet LE, Beekman R, Amadiume N, Belman AL, Krupp LB. The Symbol Digit Modalities Test is an effective cognitive screen in pediatric onset multiple sclerosis (MS). Journal of the neurological sciences. 2014;341(1-2):79-84.

96. Van Schependom J, D'Hooghe M B, Cleynhens K, D'Hooge M, Haelewyck MC, De Keyser J, et al. The Symbol Digit Modalities Test as sentinel test for cognitive impairment in multiple sclerosis. European journal of neurology. 2014;21(9):1219-25.
97. Parmenter BA, Weinstock-Guttman B, Garg N, Munschauer F, Benedict RH. Screening for cognitive impairment in multiple sclerosis using the symbol digit modalities test. Multiple sclerosis. 2007;13(1):52-7.
98. Hobart J, Lamping D, Fitzpatrick R, Riazi A, Thompson A. The Multiple Sclerosis Impact Scale (MSIS-29): a new patient-based outcome measure. Brain. 2001;124:962-73.
99. Tewarie P, Balk L, Costello F, Green A, Martin R, Schippling S, et al. The OSCAR-IB consensus criteria for retinal OCT quality assessment. PLoS One. 2012;7(4):e34823.
100. Cruz-Herranz A, Balk LJ, Oberwahrenbrock T, Saidha S, Martinez-Lapiscina EH, Lagreze WA, et al. The APOSTEL recommendations for reporting quantitative optical coherence tomography studies. Neurology. 2016;86(24):2303-9.
101. Ng DS, Gupta P, Tham YC, Peck CF, Wong TY, Ikram MK, et al. Repeatability of Perimacular Ganglion Cell Complex Analysis with Spectral-Domain Optical Coherence Tomography. Journal of ophthalmology. 2015;2015:605940.
102. Bland JM, Altman DG. Statistical methods for assessing agreement between two methods of clinical measurement. The Lancet. 1986;1(8476):307-10.
103. Brautaset R, Birkeldh U, Rosen R, Ramsay MW, Nilsson M. Reproducibility of disc and macula optical coherence tomography using the Canon OCT-HS100 as compared with the Zeiss Cirrus HD-OCT. European journal of ophthalmology. 2014;24(5):722-7.
104. Pierro L, Gagliardi M, Iuliano L, Ambrosi A, Bandello F. Retinal nerve fiber layer thickness reproducibility using seven different OCT instruments. Investigative ophthalmology & visual science. 2012;53(9):5912-20.
105. Wolf-Schnurrbusch UE, Ceklic L, Brinkmann CK, Iliev ME, Frey M, Rothenbuehler SP, et al. Macular thickness measurements in healthy eyes using six different optical coherence tomography instruments. Investigative ophthalmology & visual science. 2009;50(7):3432-7.
106. Savini G, Barboni P, Carbonelli M, Zanini M. The effect of scan diameter on retinal nerve fiber layer thickness measurement using stratus optic coherence tomography. Archives of ophthalmology. 2007;125(7):901-5.
107. Syc SB, Saidha S, Newsome SD, Ratchford JN, Levy M, Ford E, et al. Optical coherence tomography segmentation reveals ganglion cell layer pathology after optic neuritis. Brain. 2012;135:521-33.
108. Al-Louzi OA, Bhargava P, Newsome SD, Balcer LJ, Frohman EM, Crainiceanu C, et al. Outer retinal changes following acute optic neuritis. Multiple sclerosis. 2016;22(3):362-72.
109. Kupersmith MJ, Garvin MK, Wang JK, Durbin M, Kardon R. Retinal ganglion cell layer thinning within one month of presentation for optic neuritis. Multiple sclerosis. 2016;22(5):641-8.
110. Oberwahrenbrock T, Schippling S, Ringelstein M, Kaufhold F, Zimmermann H, Keser N, et al. Retinal damage in multiple sclerosis disease subtypes measured by high-resolution optical coherence tomography. Multiple sclerosis international. 2012;2012:530305.

111. Graham EC, You Y, Yiannikas C, Garrick R, Parratt J, Barnett MH, et al. Progressive Loss of Retinal Ganglion Cells and Axons in Nonoptic Neuritis Eyes in Multiple Sclerosis: A Longitudinal Optical Coherence Tomography Study. Investigative ophthalmology & visual science. 2016;57(4):2311-7.
112. Huang-Link YM, Fredrikson M, Link H. Benign Multiple Sclerosis is Associated with Reduced Thinning of the Retinal Nerve Fiber and Ganglion Cell Layers in Non-Optic-Neuritis Eyes. Journal of clinical neurology. 2015;11(3):241-7.
113. Walter SD, Ishikawa H, Galetta KM, Sakai RE, Feller DJ, Henderson SB, et al. Ganglion cell loss in relation to visual disability in multiple sclerosis. Ophthalmology. 2012;119(6):1250-7.
114. Evangelou N, Konz D, Esiri MM, Smith S, Palace J, Matthews PM. Size-selective neuronal changes in the anterior optic pathways suggest a differential susceptibility to injury in multiple sclerosis. Brain. 2001;124:1813-20.
115. Toledo J, Sepulcre J, Salinas-Alaman A, Garcia-Layana A, Murie-Fernandez M, Bejarano B, et al. Retinal nerve fiber layer atrophy is associated with physical and cognitive disability in multiple sclerosis. Multiple sclerosis. 2008;14(7):906-12.
116. Garcia-Martin E, Polo V, Larrosa JM, Marques ML, Herrero R, Martin J, et al. Retinal layer segmentation in patients with multiple sclerosis using spectral domain optical coherence tomography. Ophthalmology. 2014;121(2):573-9.
117. Garcia-Martin E, Ara JR, Martin J, Almarcegui C, Dolz I, Vilades E, et al. Retinal and Optic Nerve Degeneration in Patients with Multiple Sclerosis Followed up for 5 Years. Ophthalmology. 2017;124(5):688-96.
118. Lange AP, Zhu F, Sayao AL, Sadjadi R, Alkabie S, Traboulsee AL, et al. Retinal nerve fiber layer thickness in benign multiple sclerosis. Multiple sclerosis. 2013;19(10):1275-81.
119. Coric D, Balk LJ, Verrijp M, Eijlers A, Schoonheim MM, Killestein J, et al. Cognitive impairment in patients with multiple sclerosis is associated with atrophy of the inner retinal layers. Multiple sclerosis. 2017;24(2):158-66.